

RESEARCH ARTICLE

# The *Candida albicans* Histone Acetyltransferase Hat1 Regulates Stress Resistance and Virulence via Distinct Chromatin Assembly Pathways

Michael Tscherner<sup>1</sup>, Florian Zwolanek<sup>1</sup>, Sabrina Jenull<sup>1</sup>, Fritz J. Sedlazeck<sup>2#a</sup>, Andriy Petryshyn<sup>1</sup>, Ingrid E. Frohner<sup>1</sup>, John Mavrianos<sup>3</sup>, Neeraj Chauhan<sup>3</sup>, Arndt von Haeseler<sup>2</sup>, Karl Kuchler<sup>1\*</sup>

**1** Department for Medical Biochemistry, Medical University of Vienna, Max F. Perutz Laboratories, Campus Vienna Biocenter, Vienna, Austria, **2** Center for Integrative Bioinformatics Vienna, Max F. Perutz Laboratories, University of Vienna, Medical University of Vienna, Campus Vienna Biocenter, Vienna, Austria, **3** Public Health Research Institute, New Jersey Medical School - Rutgers, The State University of New Jersey, Newark, New Jersey, United States of America

#a Current address: Cold Spring Harbor Laboratory, Cold Spring Harbor, New York, United States of America

\* [karl.kuchler@meduniwien.ac.at](mailto:karl.kuchler@meduniwien.ac.at)



CrossMark  
click for updates

 OPEN ACCESS

**Citation:** Tscherner M, Zwolanek F, Jenull S, Sedlazeck FJ, Petryshyn A, Frohner IE, et al. (2015) The *Candida albicans* Histone Acetyltransferase Hat1 Regulates Stress Resistance and Virulence via Distinct Chromatin Assembly Pathways. PLoS Pathog 11(10): e1005218. doi:10.1371/journal.ppat.1005218

**Editor:** Damian J Krysan, University of Rochester, UNITED STATES

**Received:** July 15, 2015

**Accepted:** September 21, 2015

**Published:** October 16, 2015

**Copyright:** © 2015 Tscherner et al. This is an open access article distributed under the terms of the [Creative Commons Attribution License](https://creativecommons.org/licenses/by/4.0/), which permits unrestricted use, distribution, and reproduction in any medium, provided the original author and source are credited.

**Data Availability Statement:** Data have been deposited at the Gene Expression Omnibus (GEO) under accession number GSE73409.

**Funding:** This work was supported by a grant from the Austrian Science Fund (Project FWF-P-25333) to KK, and in part by funds from a joint research cluster of the University of Vienna and the Medical University of Vienna to KK and AvH. NC was supported by the National Institutes of Health (NIH RO1A146223). The funders had no role in study design, data collection

## Abstract

Human fungal pathogens like *Candida albicans* respond to host immune surveillance by rapidly adapting their transcriptional programs. Chromatin assembly factors are involved in the regulation of stress genes by modulating the histone density at these loci. Here, we report a novel role for the chromatin assembly-associated histone acetyltransferase complex NuB4 in regulating oxidative stress resistance, antifungal drug tolerance and virulence in *C. albicans*. Strikingly, depletion of the NuB4 catalytic subunit, the histone acetyltransferase Hat1, markedly increases resistance to oxidative stress and tolerance to azole antifungals. Hydrogen peroxide resistance in cells lacking Hat1 results from higher induction rates of oxidative stress gene expression, accompanied by reduced histone density as well as subsequent increased RNA polymerase recruitment. Furthermore, *hat1*Δ/Δ cells, despite showing growth defects *in vitro*, display reduced susceptibility to reactive oxygen-mediated killing by innate immune cells. Thus, clearance from infected mice is delayed although cells lacking Hat1 are severely compromised in killing the host. Interestingly, increased oxidative stress resistance and azole tolerance are phenocopied by the loss of histone chaperone complexes CAF-1 and HIR, respectively, suggesting a central role for NuB4 in the delivery of histones destined for chromatin assembly via distinct pathways. Remarkably, the oxidative stress phenotype of *hat1*Δ/Δ cells is a species-specific trait only found in *C. albicans* and members of the CTG clade. The reduced azole susceptibility appears to be conserved in a wider range of fungi. Thus, our work demonstrates how highly conserved chromatin assembly pathways can acquire new functions in pathogenic fungi during coevolution with the host.

and analysis, decision to publish, or preparation of the manuscript.

**Competing Interests:** The authors have declared that no competing interests exist.

## Author Summary

*Candida albicans* is the most prevalent fungal pathogen infecting humans, causing life-threatening infections in immunocompromised individuals. Host immune surveillance imposes stress conditions upon *C. albicans*, to which it has to adapt quickly to escape host killing. This can involve regulation of specific genes requiring disassembly and reassembly of histone proteins, around which DNA is wrapped to form the basic repeat unit of eukaryotic chromatin—the nucleosome. Here, we discover a novel function for the chromatin assembly-associated histone acetyltransferase complex NuB4 in oxidative stress response, antifungal drug tolerance as well as in fungal virulence. The NuB4 complex modulates the induction kinetics of hydrogen peroxide-induced genes. Furthermore, NuB4 negatively regulates susceptibility to killing by immune cells and thereby slowing the clearing from infected mice *in vivo*. Remarkably, the oxidative stress resistance seems restricted to *C. albicans* and closely related species, which might have acquired this function during coevolution with the host.

## Introduction

Eukaryotic chromatin is densely packed with the nucleosome being its basic repeating unit [1]. This structure represents a barrier for enzymes reading or modifying genomic DNA. Thus, disassembly and reassembly of histones, the core components of nucleosomes, is essential for various biological processes, including transcription, replication and DNA repair [2–7]. Two key players in the deposition of newly synthesized histones into chromatin are type B histone acetyltransferases (HATs) and histone chaperones. Type B HATs specifically acetylate free histones immediately after synthesis and show at least partial cytoplasmic localization. Hat1 was the first type B HAT identified and was found conserved throughout the eukaryotic kingdom [8,9]. Together with the Hat2 subunit (RbAp46/48 in higher eukaryotes), Hat1 acetylates histone H4 at lysine 5 and 12 in *Saccharomyces cerevisiae* and *Candida albicans* [9,10]. After binding of an additional subunit in the nucleus, the so-called NuB4 complex is formed, which is responsible for histone deposition at sites of DNA damage [11,12]. Rtt109 is another fungal-specific Type B HAT involved in DNA damage repair and associated histone deposition by acetylating free histone H3 at lysine 56 [2,13]. Interestingly, telomeric silencing is also defective in *S. cerevisiae* and *Schizosaccharomyces pombe hat1Δ* mutants [14,15]. Thus, Hat1 appears to be also involved in the generation or maintenance of repressive chromatin structures.

Hat1 operates with various histone chaperones [16–18]. This class of proteins is able to bind histones thereby avoiding unspecific interactions with DNA and facilitating correct incorporation into nucleosomes [19]. Two main chromatin assembly pathways include the hallmark histone chaperone complexes CAF-1 and HIR. While CAF-1 is well known to function in replication-coupled chromatin assembly, recent reports indicate also a role in transcription regulation [20–22]. In contrast, HIR is involved in replication-independent chromatin assembly and acts as a repressor of histone genes outside of S-phase [23]. Of note, Hat1 was found in complexes together with CAF-1 or HIR, thus suggesting a central role in the delivery of newly synthesized histones for incorporation via distinct pathways [16,18].

The opportunistic human fungal pathogen *Candida albicans* is the most frequent cause of *Candida*-derived invasive infections [24]. *Candida* spp. can cause diseases ranging from chronic mucocutaneous to life-threatening systemic infections in immunocompromised patients. *C. albicans* belongs to the CTG clade, a group of closely related species which translate the CUG codon as serine instead of leucine [25]. During the infection process, *C. albicans*

encounters various environmental stress conditions, including reactive oxygen species (ROS) produced by innate immune cells such as macrophages, dendritic cells or neutrophils dedicated to kill invading pathogens [26]. Furthermore, treatment with antifungal agents such as azoles, which inhibit fungal ergosterol biosynthesis and are commonly used to treat *Candida* infections, also represents severe stress to the pathogen [27]. At least two major mechanisms are therefore essential for *C. albicans* to be able to survive under these conditions: the fungus has to be able to repair damaged cellular components efficiently, and it has to respond rapidly by adapting transcriptional programs to counteract immune defense [28–32]. Changes in chromatin structure are involved in both mechanisms. Disassembly and reassembly of histones is required for efficient repair of DNA damage [2,7]. Furthermore, transcriptional modulation is intimately linked to the histone density at the corresponding loci [6,33–35]. Interestingly, several studies reported functions of chromatin-remodeling factors in the regulation of stress-responsive genes [33,36–38]. For instance, incorporation of histones into chromatin is particularly important for efficient gene repression, as the increase of histone density impairs binding of activators and inhibits RNA polymerase progression [6,39,40].

We have recently shown that *C. albicans* NuB4 complex is required for efficient repair of DNA damage resulting from endogenous or exogenous impact [10]. Here, we report a novel function for NuB4 in the negative regulation of oxidative stress resistance and azole tolerance. The Hat1 component of NuB4 acts in concert with distinct chromatin assembly pathways, which is independent of its conserved role in DNA damage repair. We show that the loss of the NuB4 complex markedly increases oxidative stress resistance through an accelerated induction of oxidative stress genes. Furthermore, this renders the pathogen resistant to killing by innate immune cells and promotes persistence of a *hat1Δ/Δ* mutant in a murine infection model. Interestingly, loss of Cac2, a subunit of the CAF-1 histone chaperone complex, mimics the oxidative stress resistance phenotype of *hat1Δ/Δ* cells. Furthermore, transcriptional profiling by RNA-Seq confirms overlapping functions of NuB4 and CAF-1 in *C. albicans*. Moreover, we also discover a novel role for NuB4 requiring the HIR complex for the negative regulation of azole tolerance in *C. albicans*. Interestingly, whereas the oxidative stress phenotype of *hat1Δ/Δ* cells has exclusively evolved in the *Candida* CTG clade, the reduced azole susceptibility seems to be conserved in a wider range of fungal species. Thus, our work demonstrates how highly conserved chromatin assembly pathways can acquire new functions, as for example in pathogenic fungi during coevolution with the host. Thus, host-specific immune defense mechanisms can act as drivers of evolutionary adaptation, enabling pathogens to cope with specific stress conditions.

## Results

### Deletion of NuB4 components increases H<sub>2</sub>O<sub>2</sub> resistance and azole tolerance

In a previous study, we identified the *C. albicans* NuB4 complex being essential for efficient repair of both exogenous and endogenous DNA damage [10]. *C. albicans* DNA damage repair mutants show increased susceptibility to ROS produced by immune cells [30]. Therefore, we asked if inactivation of the NuB4 complex would render this pathogen hypersusceptible to H<sub>2</sub>O<sub>2</sub>. Surprisingly, however, deletion of *HAT1*, *HAT2* or both genes increased the resistance to H<sub>2</sub>O<sub>2</sub> as determined by spot dilution assays (Fig 1A). Importantly, reintegration of *HAT1* or *HAT2* at its endogenous locus fully restored the wild-type phenotype (Fig 1A).

Due to this unexpected resistance phenotype, we subjected the *hat1Δ/Δ* mutant to phenotypic analysis by applying a set of different stress conditions including cell wall stress (Calcofluor White, Congo Red), osmotic stress (NaCl), oxidative stress (*tert*-Butyl hydroperoxide

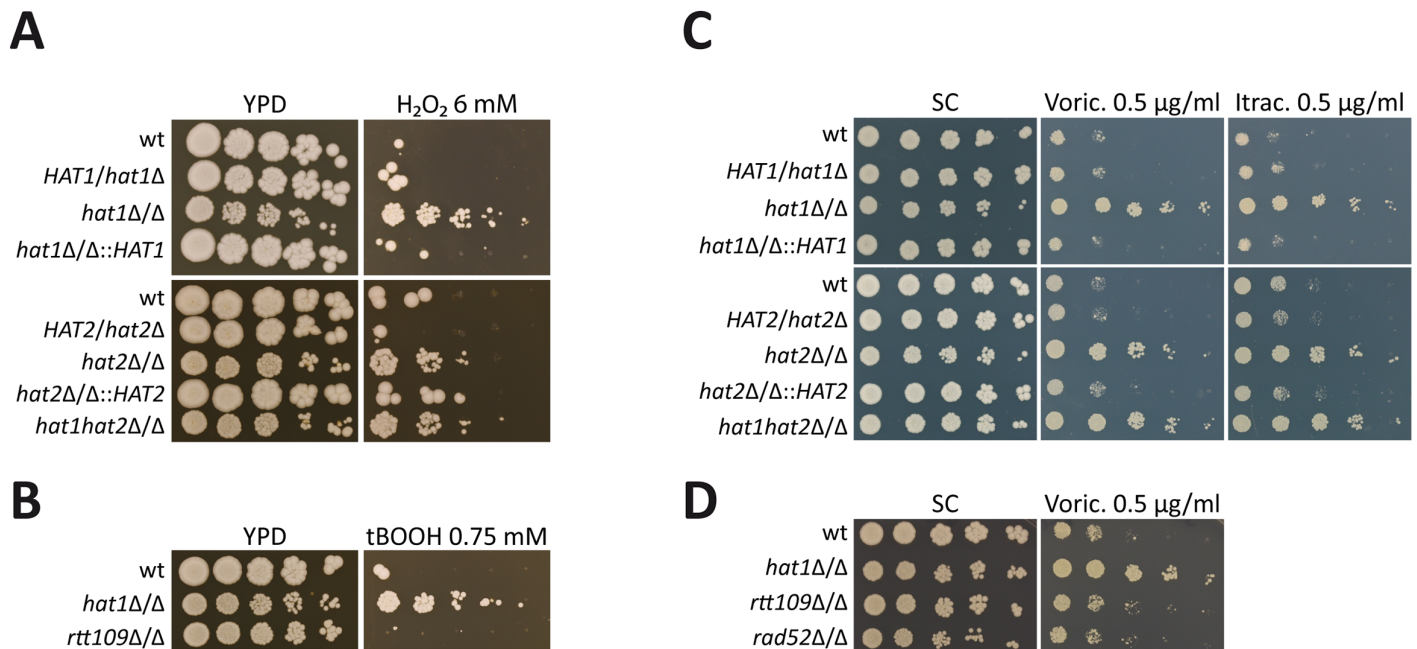


**Fig 1. Deletion of *HAT1* and *HAT2* increases oxidative stress resistance and azole tolerance.** (A) Cells lacking Hat1 or Hat2 show increased resistance to H<sub>2</sub>O<sub>2</sub>. Lack of both genes mimics the corresponding single deletion strains. (B) Deletion of *HAT1* increases resistance to *tert*-butyl hydroperoxide (tBOOH). Lack of Rtt109 does not affect tBOOH sensitivity. (C) Loss of Hat1 causes reduced susceptibility to voriconazole (Voric.) and itraconazole (Itrac.). Deletion of *HAT2* or *HAT1* and *HAT2* mimics loss of Hat1. (D) Deletion of *RTT109* or *RAD52* does not increase voriconazole tolerance. (A–D) Fivefold serial dilutions of the indicated strains were spotted on agar plates containing the indicated substances and pictures were taken after incubation at 30°C for 3 days.

doi:10.1371/journal.ppat.1005218.g001

(tBOOH), diamide), heavy metal stress (CdCl<sub>2</sub>), as well as antifungal drugs (Voriconazole, Itraconazole, Amphotericin B). For most conditions, we did not observe any difference between the wild-type and the *hat1Δ/Δ* strain (S1A Fig). However, lack of Hat1 markedly increased resistance to the oxidizing agents tBOOH and diamide, indicating a specific role for Hat1 in the regulation of oxidative stress resistance (Fig 1B and S1B Fig).

Interestingly, we also observed that deletion of *HAT1* increased tolerance to different azole drugs (Fig 1C). Azoles represent a widely used class of antifungals targeting the lanosterol 14- $\alpha$ -demethylase, thereby blocking fungal ergosterol biosynthesis. Furthermore, deletion of *HAT2* or *HAT1* and *HAT2* mimicked deletion of *HAT1* and reintegration of both genes at their endogenous loci fully restored the wild-type phenotype (Fig 1C). To confirm that the observed resistance phenotypes are independent of the NuB4 function in DNA damage repair, we determined sensitivities of different DNA damage repair mutants to H<sub>2</sub>O<sub>2</sub> and voriconazole. Importantly, neither deletion of the gene encoding the histone H3 specific acetyltransferase Rtt109 nor the absence of the repair protein Rad52 yielded in comparable oxidative stress or voriconazole phenotypes (Fig 1B, 1D and S1C Fig). Hence, not all defects in DNA repair lead to oxidative stress resistance. These data suggest that Hat1 has an additional and novel function in *C. albicans* in the regulation of oxidative stress resistance and antifungal drug tolerance.

### Inactivation of chromatin assembly pathways mimics lack of Hat1

Hat1 is involved in the deposition of histone H3–H4 dimers at sites of DNA damage and in heterochromatic regions in different species [14,41–43]. Different histone chaperones are responsible for the incorporation of histones into nucleosomes via distinct chromatin assembly

pathways [20,44–47]. We hypothesized that a defect in chromatin assembly is causing the observed resistance phenotypes. Therefore, we created deletion mutants of a set of genes encoding histone chaperones or histone chaperone complex components known to interact or copurify with Hat1 or to regulate gene expression in other species (Table 1). Genes were deleted in wild-type cells as well as in a *hat1Δ/Δ* background and sensitivities to H<sub>2</sub>O<sub>2</sub> and voriconazole were tested.

Strikingly, lack of *CAC2*, a subunit of the CAF-1 histone chaperone complex, also strongly increased resistance to H<sub>2</sub>O<sub>2</sub> and tBOOH (Fig 2A and S1D Fig). Furthermore, a quantification of H<sub>2</sub>O<sub>2</sub> resistance by determination of the survival rate in liquid culture confirmed this result (Fig 2B). Interestingly however, spot dilution assays suggested a minor effect on azole susceptibility of *cac2Δ/Δ* cells (Fig 2C). By contrast, deletion of *HIR1*, a component of the HIR histone chaperone complex, dramatically increased tolerance to voriconazole, but did not alter H<sub>2</sub>O<sub>2</sub> susceptibility (Fig 2A and 2C). Importantly, *HAT1* and *HIR1* are epistatic, since a double deletion strain failed to show increased azole resistance when compared to the corresponding single deletions based on spot dilution assays and growth inhibition in liquid culture (Fig 2C and 2D).

Deletion of *RTT106* did not alter susceptibility to H<sub>2</sub>O<sub>2</sub> and voriconazole (Fig 2A and 2C). Unfortunately, we and others were unable to construct homozygous deletion mutants for *ASF1* and *SPT16*, indicating that they might be essential [51,52]. We also included the *C. albicans* mutant lacking the histone chaperone Spt6 [53]. Similar to *HAT1*, deletion of *SPT6* increased H<sub>2</sub>O<sub>2</sub> resistance (Fig 2E and 2F). However, a reliable and accurate determination of azole sensitivities of the homozygous *spt6Δ/Δ* mutant was not possible due to its pronounced slow-growth phenotype. Of note, deletion of one *SPT6* allele also decreased susceptibility to voriconazole (Fig 2F).

In a previous study, we showed that reducing histone H4 gene dosage mimics the genetic deletion of *HAT1* with respect to sensitivity to genotoxic stress [10]. Furthermore, a common set of genes is differentially regulated upon depletion of histone H4 and deletion of *CAC2* in *S. cerevisiae* [37]. Thus, we determined the effect of histone H4 reduction on oxidative stress and azole susceptibility. Interestingly, strains harboring a single copy of the histone H4 gene remaining also displayed increased H<sub>2</sub>O<sub>2</sub> resistance and slightly elevated tolerance to voriconazole (Fig 2G). In summary, these data indicate that defects in distinct *C. albicans* chromatin assembly pathways can alter susceptibilities to H<sub>2</sub>O<sub>2</sub> and voriconazole, thus regulating oxidative stress response and tolerance to azole antifungals, respectively.

## Oxidative stress resistance upon loss of Hat1 is restricted to CTG clade species

Next, we wanted to determine if the role of Hat1 in the regulation of oxidative stress resistance and azole tolerance is conserved in other fungal species. Therefore, we analyzed the effect of *HAT1* deletion on H<sub>2</sub>O<sub>2</sub> and voriconazole susceptibility in the distantly related fungi *Saccharomyces cerevisiae*, *Candida glabrata* and *Schizosaccharomyces pombe*. However, loss of Hat1 did not lead to increased resistance to H<sub>2</sub>O<sub>2</sub> in any of these species (Fig 3A). Furthermore, lack of Hat1 failed to lower voriconazole sensitivity in *S. cerevisiae* and *C. glabrata* (Fig 3B), but increased azole tolerance in *S. pombe* (Fig 3Bc).

Based on these results, we speculated that Hat1 might have acquired a role in the regulation of oxidative stress resistance only later in evolution. To prove this, we constructed homozygous *HAT1* deletion mutants in the more closely related CTG clade members *Candida parapsilosis* and *Candida tropicalis* and determined their H<sub>2</sub>O<sub>2</sub> sensitivity. Strikingly, lack of Hat1 decreased the susceptibility to H<sub>2</sub>O<sub>2</sub> (Fig 3C) and increased tolerance to voriconazole in both

**Table 1. Selected histone chaperone genes for deletion in *C. albicans*.**

Gene Name	ORF number	Complex	Deleted	Reference
<i>CAC2</i>	orf19.6670	CAF-1	+	[16,48]
<i>HIR1</i>	orf19.2099	HIR/HIRA	+	[18]
<i>RTT106</i>	orf19.1177		+	[38,49]
<i>ASF1</i>	orf19.3715		-	[16,17]
<i>SPT16</i>	orf19.2884	FACT	-	[50]
<i>SPT6</i>	orf19.7136		+	[33,35]

Histone chaperone genes chosen for deletion are listed. + indicates successful deletion;—indicates that no deletion mutant was obtained.

doi:10.1371/journal.ppat.1005218.t001

species (Fig 3D). Thus, the role of Hat1 in regulating oxidative stress resistance appears specific for *C. albicans* and related species within the CTG clade, while the function in azole tolerance is present in a wider range of fungal species.

### Loss of Hat1 primarily affects transcriptional repression

To investigate the effect of *HAT1* deletion during normal growth, and to elucidate the mechanism of oxidative stress resistance in the *hat1Δ/Δ* mutant, we determined transcriptional profiles of cells during the logarithmic growth phase and upon H<sub>2</sub>O<sub>2</sub> treatment. Therefore, we performed RNA sequencing (RNA-Seq) analysis on cells before and after exposure to 1.6 mM H<sub>2</sub>O<sub>2</sub> for 30 minutes. Importantly, no loss of viability was observed even after 1 hour treatment at this peroxide concentration (S2A Fig). Furthermore, transcriptional profiles were also determined for the *cac2Δ/Δ* strain, since this mutant also showed an oxidative stress resistance phenotype. In addition, we included *rtt109Δ/Δ* cells as a control, as it mimics lack of Hat1 concerning morphology and accumulation of DNA damages [10,30], yet shows wild-type susceptibility to H<sub>2</sub>O<sub>2</sub> (S1C Fig).

RNA-Seq analysis of logarithmically growing cells showed that genetic removal of *HAT1* primarily upregulates a large number of genes. We found 743 genes at least 2-fold induced and 209 genes 2-fold repressed in the *hat1Δ/Δ* mutant when compared to the wild-type. Furthermore, the amplitude of gene repression was clearly lower when compared to the upregulation of genes, implying that Hat1 exerts primarily repressing rather than activating functions (Fig 4A). Also for the *cac2Δ/Δ* and *rtt109Δ/Δ* mutants, we observed an almost exclusive upregulation of gene expression when compared to the wild-type (Fig 4B and 4C). However, lack of Cac2 or Rtt109 had a less pronounced effect concerning the number of upregulated genes when compared to the loss of Hat1. In the *cac2Δ/Δ* and the *rtt109Δ/Δ* strains, 464 and 243 genes were transcriptionally upregulated, respectively. Comparison of regulated genes in the *hat1Δ/Δ*, the *cac2Δ/Δ* and the *rtt109Δ/Δ* mutants revealed large overlaps between all datasets (Fig 4D) with 123 genes upregulated in all three mutants. Interestingly, the majority of upregulated genes in the *cac2Δ/Δ* mutant were also induced in the *hat1Δ/Δ* strain. As expected, we also detected a large overlap between the *hat1Δ/Δ* and the *rtt109Δ/Δ* strain, since both mutants share functions in DNA damage repair and cell morphology [10,30].

Following H<sub>2</sub>O<sub>2</sub> treatment, downregulated genes in the *hat1Δ/Δ* mutant increased to 459 when compared to the wild-type, although under these conditions the majority of differentially regulated genes remain up (907). The comparison of upregulated genes in the *hat1Δ/Δ*, the *cac2Δ/Δ* and the *rtt109Δ/Δ* mutants again revealed large overlaps between the three datasets (Fig 4E). Similar to the untreated condition, most genes with higher expression levels in the *cac2Δ/Δ* strain were also upregulated in the *hat1Δ/Δ* mutant, suggesting redundant functions

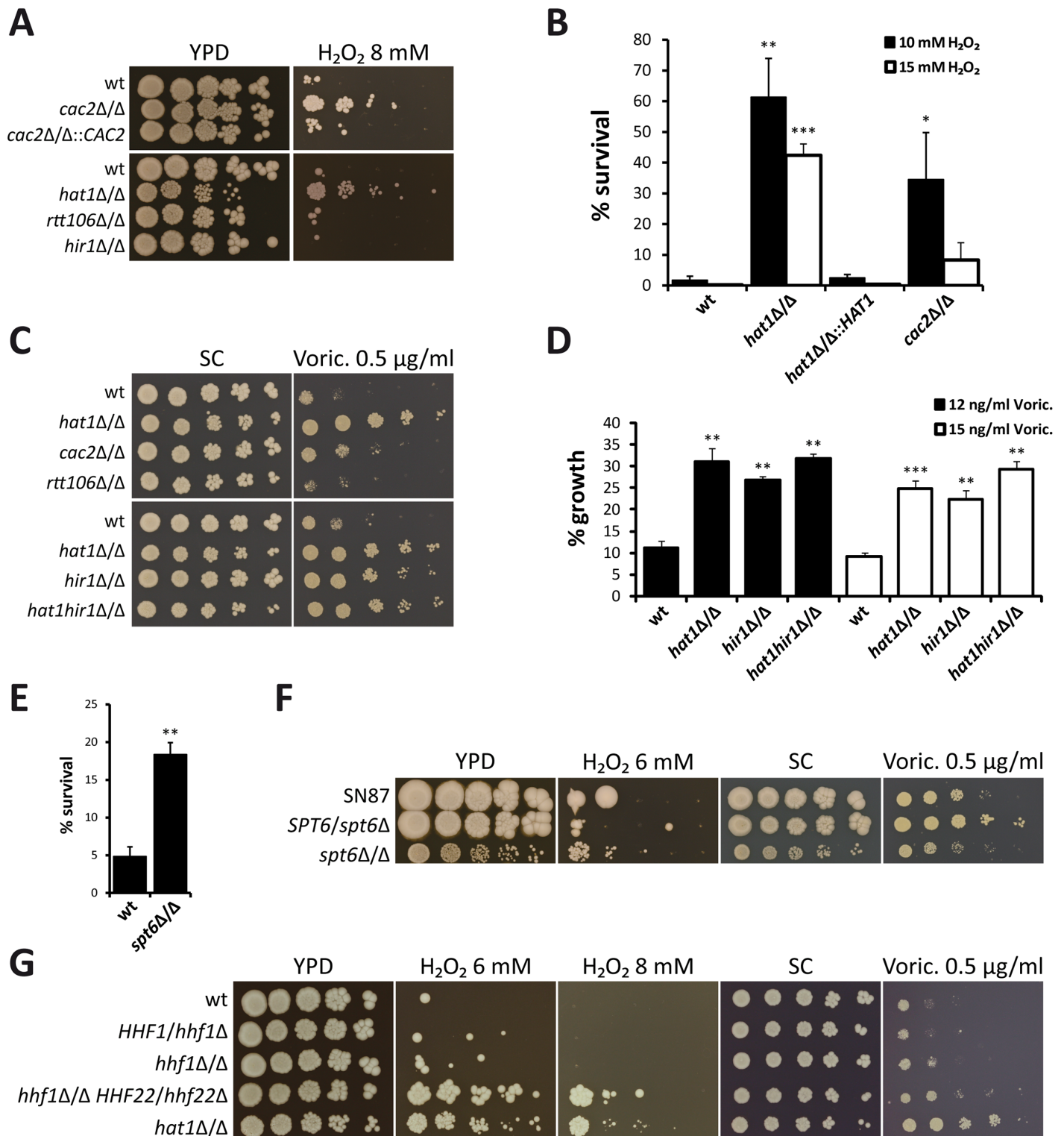


**Fig 2. Lack of histone chaperones mimics deletion of HAT1.** (A) Loss of Cac2 increases H<sub>2</sub>O<sub>2</sub> resistance. Deletion of *RTT106* or *HIR1* does not affect susceptibility to hydrogen peroxide. Fivefold serial dilutions of the indicated strains were spotted on agar plates containing the indicated substances and pictures were taken after incubation at 30°C for 3 days. (B) Deletion of *HAT1* or *CAC2* increases survival to transient hydrogen peroxide treatment. Exponentially growing cells were treated with the indicated concentrations of H<sub>2</sub>O<sub>2</sub> for 2 hours. Cells were plated and colonies counted after 3 days of incubation on YPD plates at 30°C to determine viability. Data are shown as mean + SD from three independent experiments. (C) Deletion of *HIR1* reduces voriconazole (Voric.) susceptibility. The *hat1hir1Δ/Δ* double deletion strain mimics lack of Hat1. Loss of *Cac2* has only a minor effect and deletion of *RTT106*

does not alter azole susceptibility. Experiment was performed as described in (A). (D) Increased azole tolerance of *hat1Δ/Δ*, *hir1Δ/Δ* and *hat1hir1Δ/Δ* was confirmed using a liquid growth inhibition assay. Logarithmically growing cells were diluted into medium containing the indicated concentrations of voriconazole (Voriconazole) and incubated at 30°C for 18 hours. OD<sub>600</sub> was determined and growth inhibition relative to untreated samples was calculated. Data are shown as mean + SD from three independent experiments. (E) Lack of Spt6 reduces H<sub>2</sub>O<sub>2</sub> susceptibility. Experiment was performed as described in (B). Cells were treated with 10 mM H<sub>2</sub>O<sub>2</sub>. Data are shown as mean + SD from two independent experiments. (F) Deletion of *SPT6* increases H<sub>2</sub>O<sub>2</sub> resistance and azole tolerance. Fivefold serial dilutions of the indicated strains were spotted on agar plates containing the indicated substances and pictures were taken after incubation at 30°C for 5 days. (G) Reduction of histone gene dosage decreases H<sub>2</sub>O<sub>2</sub> and azole susceptibility. Experiment was performed as described in (A). (B, D, E) \*P<0.05, \*\*P<0.01 and \*\*\*P<0.001 relative to the corresponding wild-type (Student's t-test).

doi:10.1371/journal.ppat.1005218.g002

of Hat1 and Cac2 in the regulation of gene expression. Furthermore, we again detected a large overlap between the *hat1Δ/Δ* and the *rtt109Δ/Δ* strains, and a common set of genes upregulated in all three mutants (Fig 4E). In addition, a large fraction of upregulated genes (449) in the *hat1Δ/Δ* mutant were repressed in the wild-type upon treatment with H<sub>2</sub>O<sub>2</sub>, indicating a defect in repression due to the lack of Hat1 (Fig 4F). However, we also detected a smaller set of upregulated genes (104) in the *hat1Δ/Δ* strain that were induced in the wild-type. Thus, lack of Hat1 primarily leads to upregulation of genes in logarithmically growing cells, as well as upon H<sub>2</sub>O<sub>2</sub> treatment indicating a repressive function of Hat1 in *C. albicans*.

In addition to protein-coding genes, we also analyzed the expression of non-coding elements, including tRNAs and small RNAs. Without treatment, most non-coding RNAs were not differentially expressed in the *hat1Δ/Δ* mutant (S1 Table). Out of 193 non-coding RNAs, 64 were repressed more than two-fold in wild-type cells upon H<sub>2</sub>O<sub>2</sub> treatment (S2B Fig). Interestingly, in the *hat1Δ/Δ* mutant, 20 of these non-coding RNAs were upregulated at least 2-fold when compared to the wild-type, again indicating impaired repression upon loss of Hat1.

## Lack of Hat1 affects specific functional gene groups

To further characterize genes upregulated upon loss of Hat1, we performed a GO term enrichment analysis. Without H<sub>2</sub>O<sub>2</sub> treatment, at least 2-fold upregulated genes in the *hat1Δ/Δ* mutant were strongly enriched for genes involved in lipid catabolic processes and oxidation-reduction processes (Fig 5A). Interestingly, the latter group includes genes encoding for proteins with functions in oxidative stress tolerance like the catalase (*CAT1*), superoxide dismutases (*SOD3-6*) and a thiol peroxidase (*orf19.87*) [26,54–56]. Preliminary proteomics data also identified this group of proteins as being upregulated in the *hat1Δ/Δ* mutant (S2C Fig). Of note, we failed to observe enrichment for DNA damage response genes most likely due to the fact that Hat1 is involved in different processes in *C. albicans*. This leads to a high number of differentially expressed genes in the mutant and could hamper detection of enriched GO groups. Therefore, we analyzed subsets of differentially expressed genes based on their expression in the three mutants. As expected, due to their DNA damage phenotype, genes significantly upregulated only in the *hat1Δ/Δ* and the *rtt109Δ/Δ* mutants were strongly enriched for DNA damage repair genes (Fig 5B). The specific overlap of regulated genes between *hat1Δ/Δ* and *cac2Δ/Δ* was still enriched for genes involved in oxidation-reduction processes and arginine metabolism, implying that Hat1 and Cac2 might be involved in the same processes (Fig 5C). Finally, we identified genes involved in mitochondrial degradation and microautophagy which were significantly upregulated only in the *hat1Δ/Δ* mutant (Fig 5D).

Next, we analyzed genes with differential expression levels in the mutants relative to the wild-type upon H<sub>2</sub>O<sub>2</sub> treatment. The whole group of genes significantly upregulated in the *hat1Δ/Δ* mutant was enriched for genes involved in rRNA processing and transport reactions (Fig 5E). We failed to detect any gene sets enriched specifically in the overlaps between the *hat1Δ/Δ* and the *rtt109Δ/Δ* or the *hat1Δ/Δ* and *cac2Δ/Δ* strains. However, we observed a strong

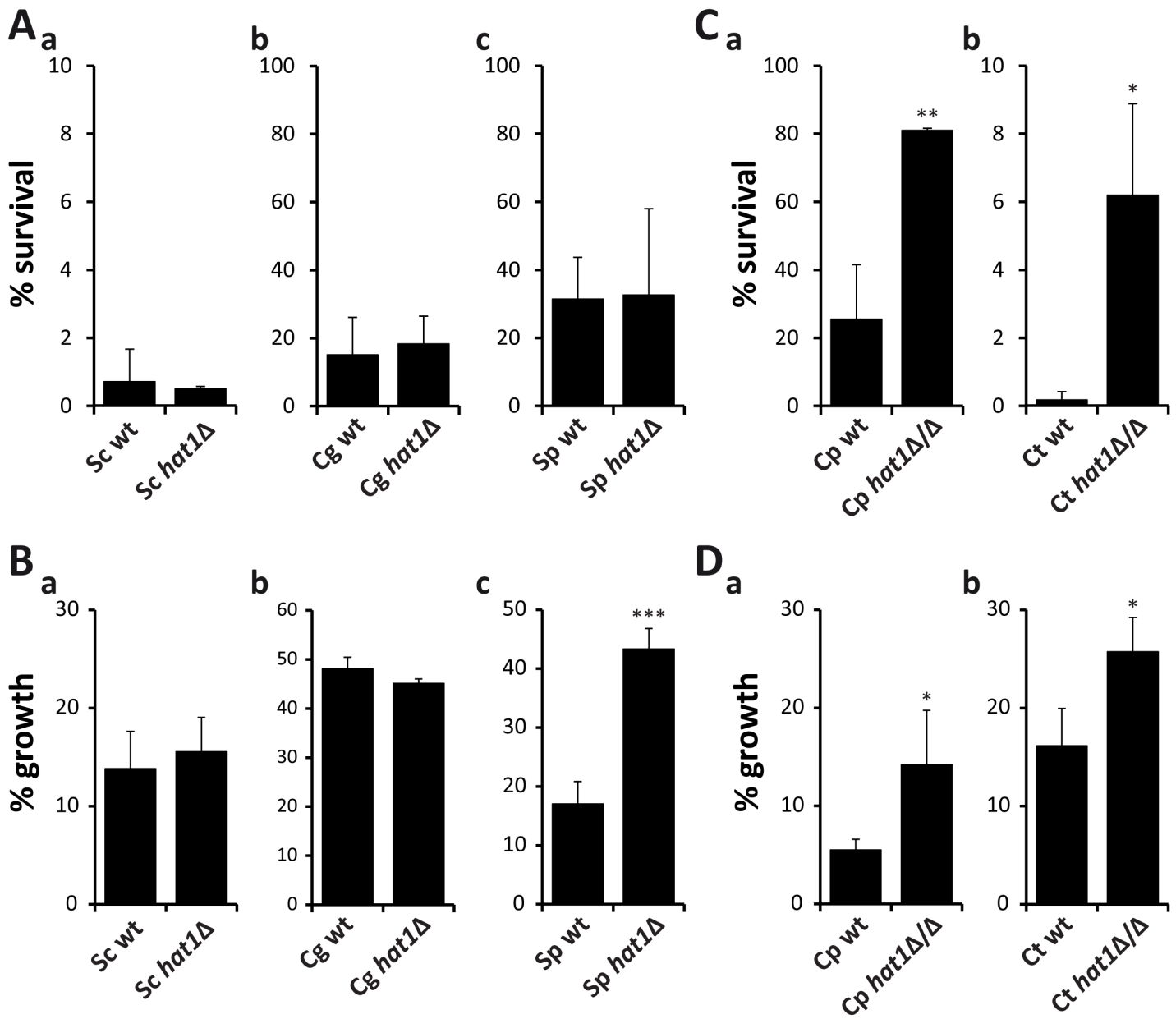


**Fig 3. Resistance phenotypes caused by loss of Hat1 are specific for *C. albicans*.** (A) Deletion of *HAT1* in *S. cerevisiae* (a), *C. glabrata* (b) and *S. pombe* (c) has no effect on H<sub>2</sub>O<sub>2</sub> resistance. Exponentially growing cells were treated with 5 mM (a), 50 mM (b) or 20 mM (c) H<sub>2</sub>O<sub>2</sub> for 2 hours. Cells were plated and colonies counted after 3 days of incubation on YPD plates at 30°C to determine viability. Data are shown as mean + SD from three independent experiments. (B) Lack of Hat1 in *S. cerevisiae* (a) and *C. glabrata* (b) does not increase azole tolerance. Deletion of Hat1 in *S. pombe* reduces susceptibility to voriconazole (c). Logarithmically growing cells were diluted into medium containing 150 ng/ml (a), 1000 ng/ml (b) or 800 ng/ml (c) voriconazole and incubated at 30°C for 24 hours. OD<sub>600</sub> was determined and growth inhibition relative to untreated samples was calculated. Data are shown as mean + SD from three independent experiments. (C) *C. parapsilosis* (a) and *C. tropicalis* (b) *hat1Δ/Δ* cells show increased resistance to H<sub>2</sub>O<sub>2</sub>. Experiment was performed as described in (A). H<sub>2</sub>O<sub>2</sub> concentrations were 50 mM (a) and 20 mM (b). (D) Loss of Hat1 in *C. parapsilosis* (a) and *C. tropicalis* (b) reduces susceptibility to voriconazole. Experiment was performed as described in (B). For *C. parapsilosis* cells were incubated for 41 hours prior to OD<sub>600</sub> measurement. Voriconazole concentrations were 50 ng/ml (a) and 200 ng/ml (b). (A-D) \*P<0.05, \*\*P<0.01 and \*\*\*P<0.001 relative to the corresponding wild-type (Student's t-test).

doi:10.1371/journal.ppat.1005218.g003

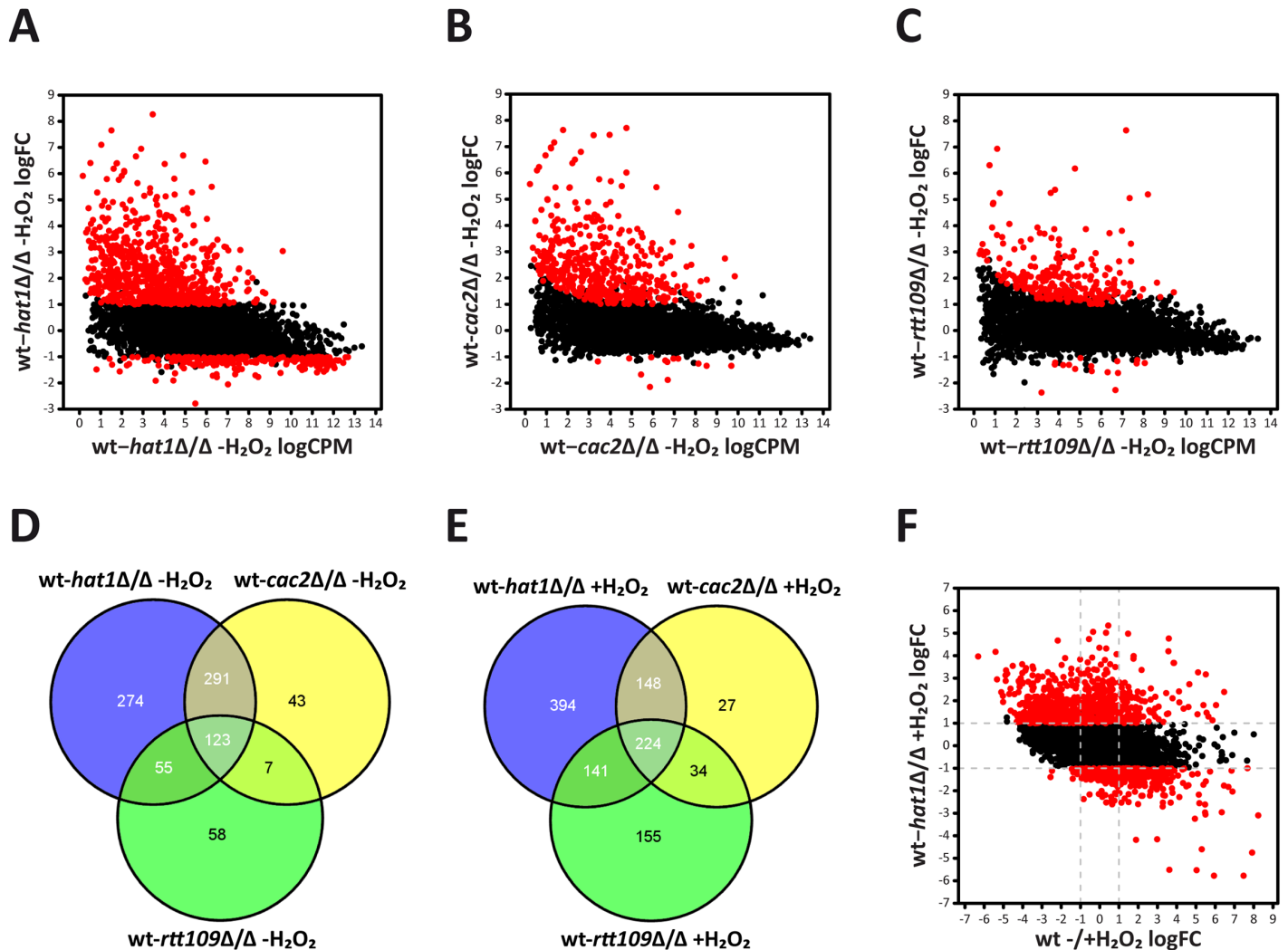


**Fig 4. Deletion of *HAT1* primarily leads to upregulation of genes.** (A) Lack of Hat1 causes mainly induction of genes in logarithmically growing cells. Each dot corresponds to one protein-coding gene. The fold change in RNA expression between untreated wild-type and *hat1Δ/Δ* cells (y-axis) is plotted against the expression level of each gene in this dataset (x-axis). Differentially expressed genes in the *hat1Δ/Δ* mutant are depicted in red. logCPM: log<sub>2</sub> counts per million reads; logFC: log<sub>2</sub> fold change; (B+C) Loss of Cac2 or Rtt109 causes almost exclusively upregulation of genes in logarithmically growing cells. Plots were created as described in (A). (D) Venn diagram showing the overlaps of upregulated genes in the *hat1Δ/Δ*, *cac2Δ/Δ* and *rtt109Δ/Δ* mutants in the absence of H<sub>2</sub>O<sub>2</sub>. (E) Venn diagram showing the overlaps of upregulated genes in the *hat1Δ/Δ*, *cac2Δ/Δ* and *rtt109Δ/Δ* mutants upon treatment with H<sub>2</sub>O<sub>2</sub>. (F) H<sub>2</sub>O<sub>2</sub> repressed genes are upregulated in the *hat1Δ/Δ* mutant upon peroxide treatment. Each dot corresponds to one protein-coding gene. The -fold change in RNA expression between H<sub>2</sub>O<sub>2</sub> treated wild-type and *hat1Δ/Δ* strains (y-axis) is plotted against the fold change between the wild-type without and with treatment (x-axis). Differentially expressed genes in the *hat1Δ/Δ* mutant are depicted in red. logFC: log<sub>2</sub> fold change; (A-F) Differentially regulated genes were defined by a fold change  $\geq 2$  and p-value  $< 0.05$ .

doi:10.1371/journal.ppat.1005218.g004

enrichment of genes involved in non-coding RNA (ncRNA)/rRNA processing and ribosome biogenesis as upregulated specifically in the *hat1Δ/Δ* mutant (Fig 5F).

In summary, loss of Hat1 mainly leads to increased expression of genes belonging to different functional groups, which is in accordance with Hat1 being involved in different processes in *C. albicans*. Furthermore, distinct functional groups affected by the loss of Hat1 are also upregulated in either the *rtt109Δ/Δ* or the *cac2Δ/Δ* strain indicating that Hat1 might function in specific processes together with Rtt109 or Cac2.

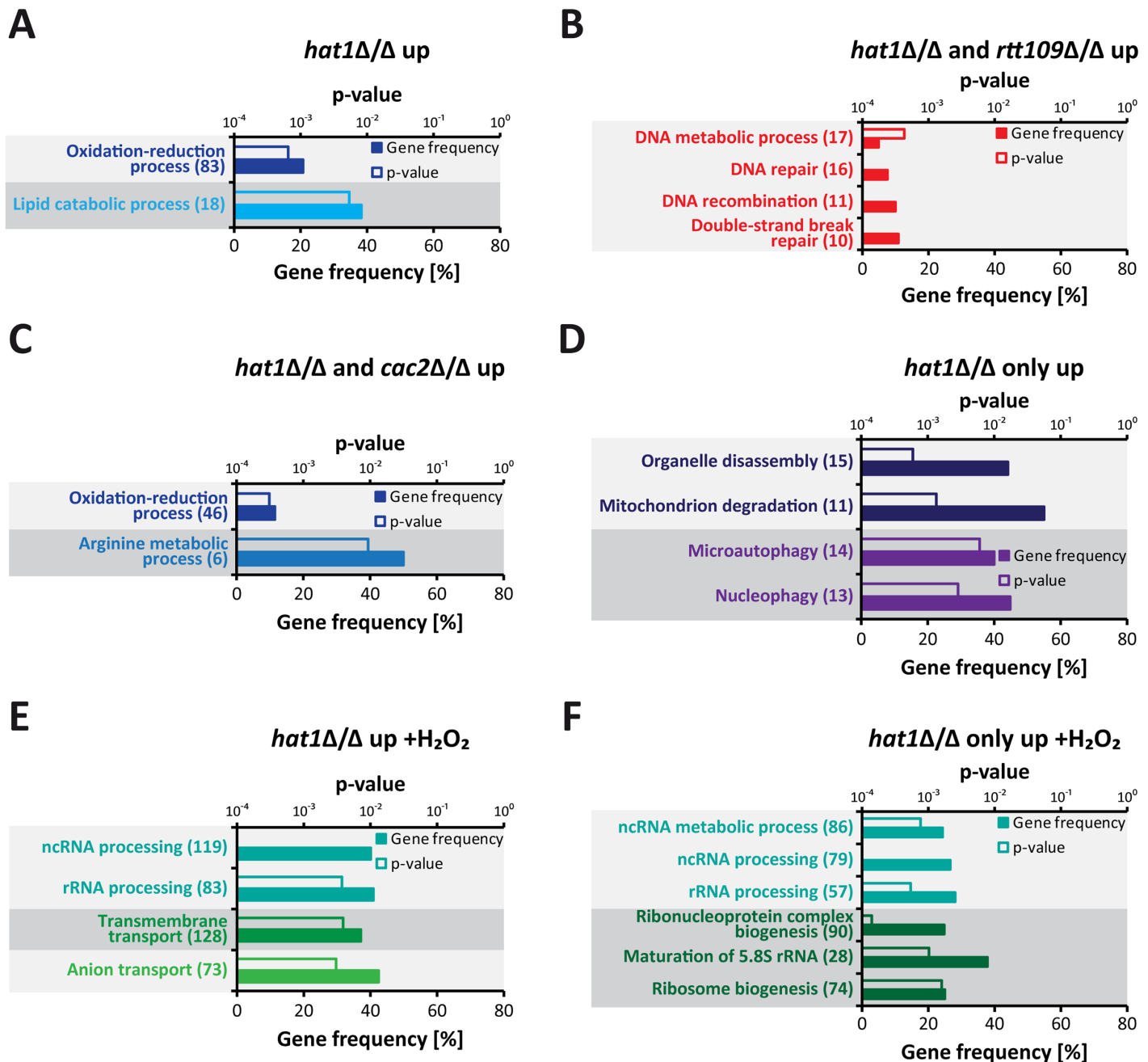


**Fig 5. Specific functional gene groups are upregulated in cells lacking Hat1.** (A) GO terms enriched among 2-fold significantly upregulated genes in logarithmically growing *hat1Δ/Δ* cells are shown. (B) The plot shows GO terms found within genes significantly upregulated in the *hat1Δ/Δ* and *rtt109Δ/Δ* strains only. (C) GO terms enriched within genes significantly upregulated in the *hat1Δ/Δ* and *cac2Δ/Δ* strains only. (D) The panel shows GO terms found among genes significantly upregulated in the *hat1Δ/Δ* mutant only and not in the *rtt109Δ/Δ* and the *cac2Δ/Δ* strains. (E) GO terms enriched among significantly upregulated genes in *hat1Δ/Δ* cells after treatment with H<sub>2</sub>O<sub>2</sub> are shown. (F) The plot shows GO terms found within genes significantly upregulated in the *hat1Δ/Δ* strain only and not in the *rtt109Δ/Δ* and the *cac2Δ/Δ* strains upon H<sub>2</sub>O<sub>2</sub> treatment. (A-F) The corresponding p-values for the enrichment (empty bars) and the percentage of genes changed within the GO group (filled bars) are presented. The absolute number of regulated genes within a GO group is presented in brackets. Groups containing identical genes are depicted in the same color. Significantly regulated genes were defined by a p-value <0.05.

doi:10.1371/journal.ppat.1005218.g005

## Deletion of *HAT1* accelerates induction of oxidative stress genes

Transcriptional profiling of *hat1Δ/Δ* and *cac2Δ/Δ* cells revealed the upregulation of various gene sets encoding for proteins involved in the response to oxidative stress. Both mutants displayed elevated transcriptional levels of *CAT1* encoding catalase, which is responsible for the decay of H<sub>2</sub>O<sub>2</sub> [54]. Of note, RT-qPCR analysis confirmed derepression of *CAT1* in *hat1Δ/Δ* and *cac2Δ/Δ* cells in the absence of H<sub>2</sub>O<sub>2</sub>. However, as expected from the RNA-Seq data, *CAT1* derepression was also observed for the *rtt109Δ/Δ* strain, which is not resistant to H<sub>2</sub>O<sub>2</sub> (S2D Fig). Thus, this moderate derepression of *CAT1* is most likely due to a general stress response in these deletion mutants.

Therefore, we investigated *CAT1* induction upon treatment with H<sub>2</sub>O<sub>2</sub>. Interestingly, lack of Hat1 as well as Cac2 caused increased *CAT1* expression, indicating that these two proteins negatively regulate the induction kinetics of *CAT1* (S2E Fig). However, induction levels in the *rtt109Δ/Δ* control strain were similar to the wild-type (S2E Fig). Since lack of Hat1 affected induction levels of *CAT1*, we investigated the induction kinetics of this gene in detail. Thus, we determined transcript levels upon treatment with H<sub>2</sub>O<sub>2</sub> over time. Interestingly, lack of Hat1 resulted in a significantly faster induction of the *CAT1* gene when compared to the wild-type (Fig 6A). Since Hat1 is involved in the deposition of histones into chromatin, we determined the effect of *HAT1* deletion on the histone density at the *CAT1* locus by chromatin immunoprecipitation (ChIP) using antibodies against histone H3. Without treatment, the *hat1Δ/Δ* mutant showed a reduced histone density at the *CAT1* promoter (Fig 6Ba). There was no difference in the occupancy in the *CAT1* coding sequence (CDS) between the mutant and the wild-type (Fig 6Bb). Interestingly, however, treatment with H<sub>2</sub>O<sub>2</sub> decreased histone density at the promoter as well as in the CDS significantly faster in *hat1Δ/Δ* cells when compared to the wild-type (Fig 6B). This explains the increased induction rate in the mutant, since nucleosomes represent a physical barrier for RNA polymerase II (RNAPII) and reduced nucleosome density can facilitate transcription [6,35,57]. Thus, lower histone density in the *hat1Δ/Δ* mutant could promote higher RNAPII processivity leading to increased mRNA production. Alternatively, elevated mRNA levels could also be due to increased RNAPII recruitment, which could be facilitated by the reduction in nucleosome density at the promoter. To clarify whether elevated mRNA levels are the consequence of increased RNAPII recruitment, we determined RNAPII levels at the *CAT1* gene using ChIP. Interestingly, we detected increased recruitment of RNAPII to the *CAT1* CDS, thus explaining the elevated mRNA levels (Fig 6C).

Notably, the oxidative stress response set upregulated in the *hat1Δ/Δ* mutant also comprised several glutathione-utilizing enzymes. Thus, we determined the induction kinetics for two of these genes upon treatment with H<sub>2</sub>O<sub>2</sub>. Similar to *CAT1*, we detected a faster induction of *GPX1* (orf19.86) encoding a glutathione peroxidase (GPx) as well as of *GST1* (orf19.3121), encoding a glutathione S-transferase (Fig 6D). In addition, we also detected increased RNAPII levels at both genes upon treatment with H<sub>2</sub>O<sub>2</sub> (Fig 6E). Notably, we observed similar hyperinduction of *GPX1* and *GST1* upon H<sub>2</sub>O<sub>2</sub> treatment for the *cac2Δ/Δ* mutant as well (Fig 6F and 6G).

Furthermore, we tested whether the increase in transcription of oxidative stress genes in the *hat1Δ/Δ* mutant is paralleled by elevated activity of the corresponding enzymes. Therefore, we prepared whole cell extracts from cells before and after 60 min exposure to H<sub>2</sub>O<sub>2</sub> and determined catalase activity as well as GPx activity spectrophotometrically. We detected elevated catalase activity in the *hat1Δ/Δ* mutant already under non-inducing conditions, albeit as expected at a low level (Fig 7A). However, H<sub>2</sub>O<sub>2</sub> treatment of *hat1Δ/Δ* cells dramatically increased catalase activity when compared to the wild-type, indicating that the mutant is more efficient in degrading hydrogen peroxide (Fig 7A). Likewise, the GPx activity assay detected

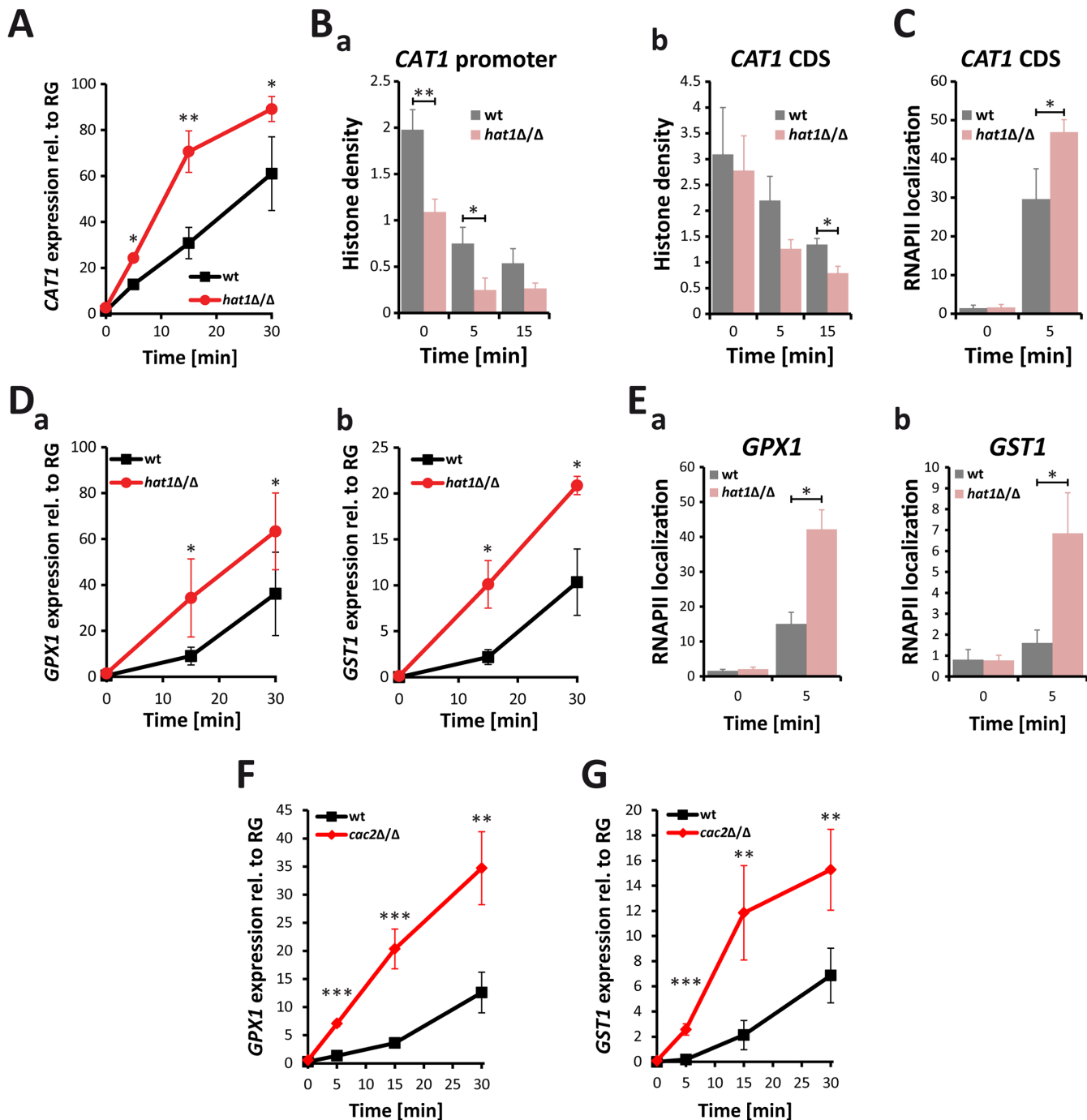


**Fig 6. Lack of Hat1 accelerates induction of oxidative stress genes.** (A) Catalase induction rate is strongly increased in *hat1Δ/Δ* cells. *CAT1* expression levels were measured by RT-qPCR after induction with 1.6 mM H<sub>2</sub>O<sub>2</sub> at the indicated time points. Transcript levels were normalized to the expression level of the reference gene (RG) *PAT1*. Data are shown as mean ± SD from 3 independent experiments. (B) Histone density at the *CAT1* locus is reduced in cells lacking Hat1. Histone H3 occupancy was determined by ChIP at the *CAT1* promoter region (a) and the CDS (b). (C) Loss of Hat1 leads to increased RNAPII recruitment at the *CAT1* locus. RNAPII levels were determined by ChIP at the *CAT1* CDS. (D) Induction rate of glutathione-utilizing enzymes is increased in *hat1Δ/Δ* cells. *GPX1* (a) and *GST1* (b) expression levels were determined by RT-qPCR at the indicated time points. Experiment was performed as described in (A). (E) Lack of Hat1 leads to increased RNAPII recruitment at the *GPX1* and *GST1* loci. RNAPII levels were determined by ChIP at the *GPX1* (a) and *GST1* (b) genes. (F+G) Loss of Cac2 increases the induction rate of both *GPX1* and *GST1* following H<sub>2</sub>O<sub>2</sub> treatment. Experimental conditions were used as described in (A).

doi:10.1371/journal.ppat.1005218.g006

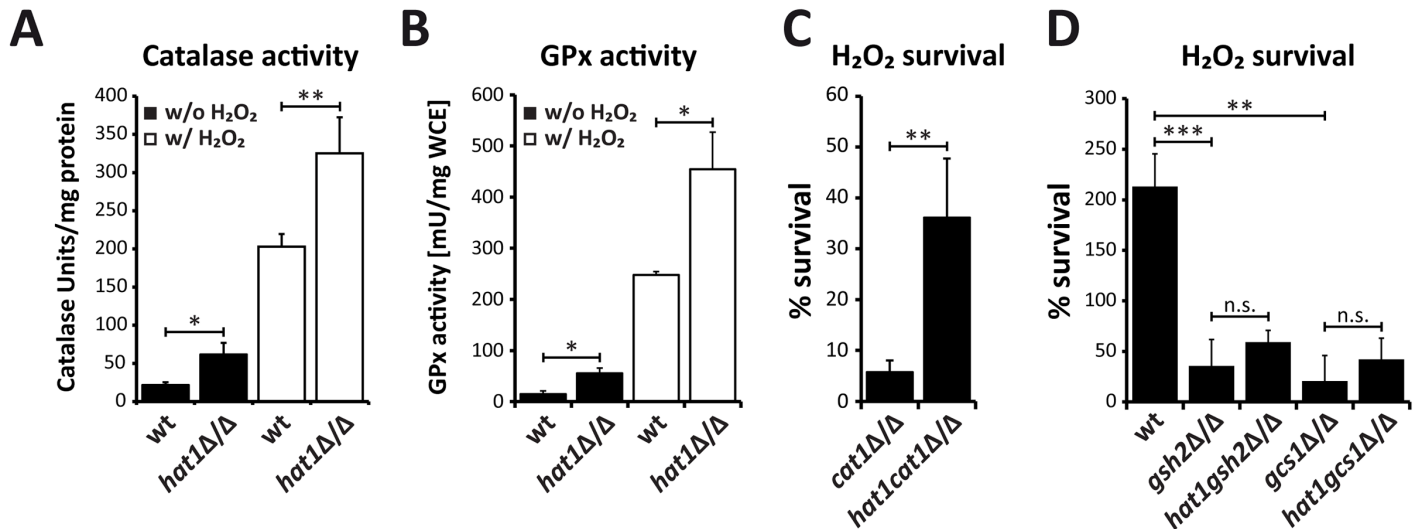


**Fig 7. Loss of Hat1 raises antioxidant enzyme activity and glutathione-mediated H<sub>2</sub>O<sub>2</sub> resistance.** (A) Faster *CAT1* induction increases catalase activity in *hat1Δ/Δ* cells. Catalase activity was determined in whole cell extracts isolated from cells before and after H<sub>2</sub>O<sub>2</sub> treatment. Data are shown as mean + SD from three independent experiments. (B) Loss of Hat1 leads to increased glutathione peroxidase activity. GPx activity was determined in whole cell extracts isolated from cells before and after H<sub>2</sub>O<sub>2</sub> treatment. Data are shown as mean + SD from two independent experiments. (C) Lack of *CAT1* does not abolish Hat1-mediated H<sub>2</sub>O<sub>2</sub> resistance. Cells of the indicated strains were treated with 1 mM H<sub>2</sub>O<sub>2</sub> for 2 hours, plated and colonies counted after 3 days of incubation on YPD plates at 30°C to determine viability. Data are shown as mean + SD from three independent experiments. (D) Depletion of glutathione biosynthesis abolishes Hat1-mediated H<sub>2</sub>O<sub>2</sub> resistance. Cells of the indicated strains were treated with H<sub>2</sub>O<sub>2</sub> for 2 hours and plated on YPD plates containing glutathione. Colonies were counted to determine viability after growth for 3 days at 30°C. Data are shown as mean + SD from three independent experiments. (A-D) n.s.: not significant, \*P<0.05, \*\*P<0.01 and \*\*\*P<0.001 relative to the corresponding control (Student's t-test).

doi:10.1371/journal.ppat.1005218.g007

some increase already under non-inducing conditions (Fig 7B), but H<sub>2</sub>O<sub>2</sub> treatment of the *hat1Δ/Δ* mutant significantly increased GPx activity (Fig 7B). These data demonstrate that the increased induction rate of oxidative stress genes in the *hat1Δ/Δ* mutant increases the activities of the enzymes encoded by the target genes.

Furthermore, to determine whether catalase hyperinduction is the main reason for the increased resistance of the *hat1Δ/Δ* mutant, we deleted the *CAT1* gene in wild-type and *hat1Δ/Δ* cells and quantified their H<sub>2</sub>O<sub>2</sub> susceptibilities. As expected, *cat1Δ/Δ* cells were highly sensitive to H<sub>2</sub>O<sub>2</sub> showing only 6% survival after treatment with a low H<sub>2</sub>O<sub>2</sub> concentration of 1 mM (Fig 7C). However, the double deletion strain maintained increased H<sub>2</sub>O<sub>2</sub> resistance when compared to the *cat1Δ/Δ* single mutant indicating that increased catalase expression is not the main reason for the hydrogen peroxide resistance of the *hat1Δ/Δ* strain (Fig 7C). To determine if increased induction of glutathione-utilizing enzymes is causing the increased H<sub>2</sub>O<sub>2</sub> resistance, we genetically depleted cells for glutathione by removing the *GSH2* and *GCS1* glutathione biosynthesis genes in wild-type and *hat1Δ/Δ* backgrounds. The first step in the synthesis of glutathione is catalyzed by the gamma-glutamylcysteine synthetase (*Gcs1*), followed by the second step carried out by the glutathione synthase (*Gsh2*). Deletion of one of these genes disrupts glutathione biosynthesis in *C. albicans* leading to glutathione auxotrophy and to increase oxidative stress sensitivity [58,59]. To determine the sensitivity to H<sub>2</sub>O<sub>2</sub> of wild-type and *hat1Δ/Δ* cells upon deletion of *GSH2* or *GCS1*, the strains were grown in the absence of glutathione and treated with H<sub>2</sub>O<sub>2</sub> for 2h. As expected, lack of *Gsh2* as well as *Gcs1* strongly increased the sensitivity to H<sub>2</sub>O<sub>2</sub> (Fig 7D). Strikingly, however, the absence of Hat1 did not significantly change H<sub>2</sub>O<sub>2</sub> resistance in the absence of *Gsh2* or *Gcs1* (Fig 7D). Thus, the data strongly suggest that H<sub>2</sub>O<sub>2</sub> resistance caused by deletion of Hat1 is mainly mediated via the glutathione system.

## Hat1 regulates ROS detoxification and neutrophil survival

The absence of Hat1 and Cac2 leads to upregulation of oxidative stress genes and resistance to hydrogen peroxide. ROS are produced by immune cells to kill *C. albicans* during the infection process. The fungus counteracts this attack by upregulating ROS detoxifying enzymes of which the superoxide dismutases Sod5 and to some extent Sod4 were shown to be essential for survival of *C. albicans* upon phagocytosis [26]. Interestingly, our RNA-Seq data not only revealed an upregulation of the catalase and glutathione-utilizing enzymes, but also markedly increased expression of genes encoding the superoxide dismutases Sod4 and Sod5 in cells lacking Hat1. The significant induction of *SOD4* and *SOD5* in the *hat1Δ/Δ* strain was also confirmed by RT-qPCR analysis (Fig 8A).

Therefore, we asked if the deletion of *HAT1* influences the ability to detoxify and survive ROS released by immune cells. ROS production during interaction of *C. albicans* with bone marrow-derived murine macrophages and bone marrow neutrophils was determined by measuring luminol dependent chemiluminescence [26]. Interestingly, deletion of *HAT1* strongly reduced total ROS levels during interaction with macrophages (Fig 8B and 8C), as well as neutrophils (S3A Fig), when compared to the wild-type. Phagocytosis is required for ROS production by the NADPH oxidase [26]. To exclude that differences in phagocytosis of the pseudohyphal *hat1Δ/Δ* cells contribute to reduced ROS levels, we performed a phagocytosis assay. However, phagocytosis was similar for the *hat1Δ/Δ* strain or wild-type (S3B Fig). Furthermore, we also determined the NADPH oxidase activation in macrophages interacting with wild-type and *hat1Δ/Δ* cells by immunoblotting. However, we observed no difference in the phosphorylation levels of the NADPH oxidase subunit p40phox upon interaction with *hat1Δ/Δ* cells or wild-type cells (S3C Fig). Therefore, reduced ROS accumulation upon interaction with *hat1Δ/Δ* cells most likely results from increased ROS detoxification by the mutant. In addition, interaction of macrophages with *rtt109Δ/Δ* cells did not lead to significant changes in the ROS levels when compared to the wild-type (Fig 8B).

Finally, we determined the resistance of *hat1Δ/Δ* cells to killing by bone marrow neutrophils. Strikingly, lack of Hat1 clearly increased the survival rate upon interaction with the immune cells. Furthermore, reintegration of *HAT1* fully restored the wild-type sensitivity (Fig 8D). These data strongly suggest that genetic removal of *HAT1* strongly promotes increased survival to neutrophil attack due to the impaired ROS accumulation.

## Cells lacking Hat1 show reduced virulence but persist in mouse kidneys

Deletion of *HAT1* causes reduced growth rate *in vitro* with morphological defects even in complete media (Fig 9A) [10], which has been shown to reduce virulence of several *C. albicans* mutants [28,30,60–63]. However, cells lacking Hat1 are also more resistant to killing by immune cells (Fig 8D). Therefore, we wanted to test how these seemingly opposing phenotypes caused by the deletion of *HAT1* affect virulence of *C. albicans*. We used a mouse model of systemic candidiasis. Infection was performed via the tail vein and fungal burdens in kidneys were followed at day 1, 3 and 7. Interestingly, after 24 hours mice infected with the *hat1Δ/Δ* mutant showed significantly reduced CFUs in the kidneys when compared to the wild-type or the restored strain (Fig 9B). However, the fungal burden of the mutant increased until day 7 after infection reaching the levels of the wild-type and the reintegrant (Fig 9B). Thus, cells lacking Hat1 are not efficiently cleared from infected mice as they are able to compensate the *in vitro* growth defect *in vivo*. To further investigate the virulence properties of the *hat1Δ/Δ* strain, we determined the survival rate of infected mice. Interestingly, 15 days post infection the majority of wild-type infected mice had died, whereas all of the mice infected with the *hat1Δ/Δ* strain were still alive (Fig 9C). Even after 32 days, only one mouse infected with the *hat1Δ/Δ* mutant

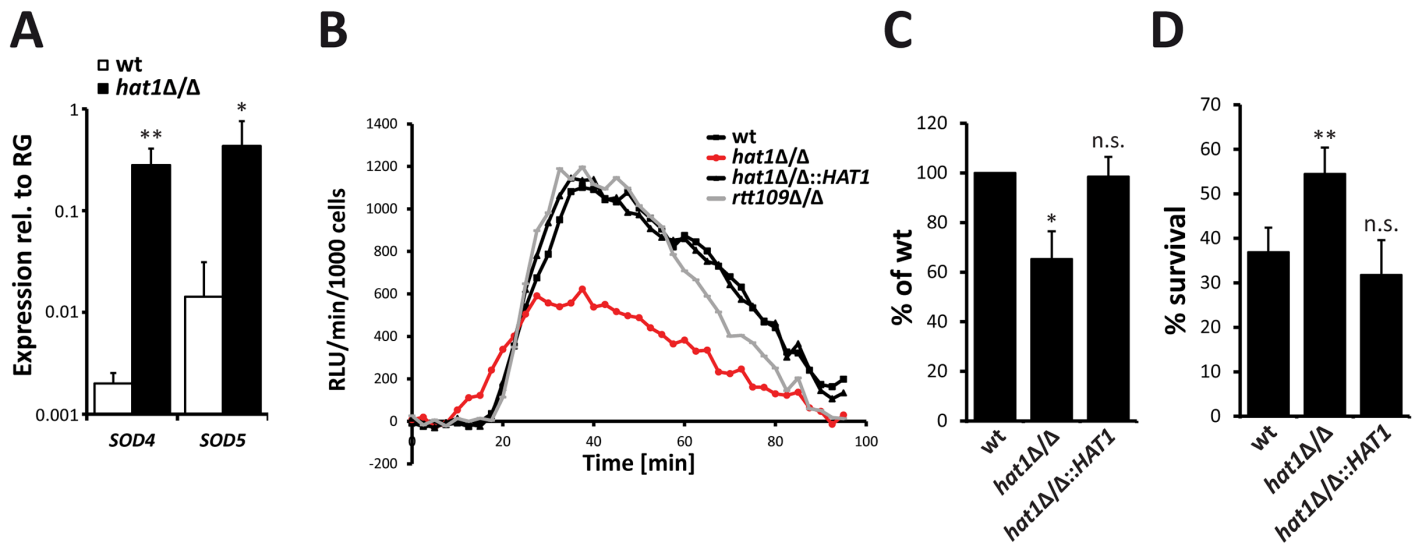


**Fig 8. Higher ROS detoxification capacity of *hat1Δ/Δ* cells causes resistance to neutrophil killing.** (A) Superoxide dismutases Sod4 and Sod5 are induced in *hat1Δ/Δ* cells. Expression levels of *SOD4* and *SOD5* in logarithmically growing cells were detected by RT-qPCR. Transcript levels were normalized to the expression level of the reference gene (RG) *RIP1*. Data are shown as mean + SD from 3 independent experiments. (B) Infection of macrophages with *hat1Δ/Δ* cells causes reduced ROS accumulation. ROS levels were determined by measuring luminol-dependent chemiluminescence [relative luciferase units (RLU) min<sup>-1</sup> per 1000 immune cells] in 2.5 min intervals during interaction of the indicated *C. albicans* strains with bone marrow-derived murine macrophages (BMDMs). One representative experiment is shown. Data were reproduced in three independent experiments. (C) Quantification of total ROS release upon interaction with BMDMs. Experiment was performed as described in (B). The area under the curve within 90 min of interaction was calculated. Data are shown as mean + SD from three independent experiments. (D) Cells lacking Hat1 show increased survival to neutrophil killing. Survival of *C. albicans* cells upon one hour interaction with murine bone marrow neutrophils was determined by plating and CFU counting. Data are shown as mean + SD from three independent experiments. (A-D) \*P<0.05, \*\*P<0.01 relative to the wild-type (Student's t-test).

doi:10.1371/journal.ppat.1005218.g008

had died. Of note, mice infected with the reintegrant showed an intermediate survival rate, which was however not significant when compared to the wild-type strain (Fig 9C). Although the majority of mice survived the infection with cells lacking Hat1, mutant cells were not cleared from the kidneys in 4 out of 5 individuals (Fig 9D). Instead, the fungal burden stayed high until the end of the experiment. Furthermore, two mice survived infection with the restored strain and for both *Candida* was not cleared (Fig 9D). Thus, again the revertant strain showed an intermediate phenotype most likely due to haploinsufficiency.

We also determined the effect of deleting *CAC2* *in vivo* using the same murine model of systemic infection as for the *hat1Δ/Δ* mutant. Interestingly enough, *cac2Δ/Δ* cells showed reduced fungal burdens at day 1 and 3 after infection. However, similar to the *hat1Δ/Δ* mutant, the strain lacking *Cac2* was also protected from clearance by the immune system, since CFUs in kidneys increased during the course of the experiment (Fig 9E). In addition, body weight measurements of infected mice revealed a striking difference between the wild-type and *hat1Δ/Δ* as well as the *cac2Δ/Δ* cells. As expected, mice infected with the wild-type rapidly lost body weight after infection. However, upon infection with the *hat1Δ/Δ* or the *cac2Δ/Δ* strain, weight loss was clearly reduced, suggesting a reduced burden to the immune system or increased tolerance to the infecting fungal strain (S4A and S4B Fig).

Nonetheless, although showing increased persistence in the host, deletion of *HAT1* strongly attenuates virulence in a mouse model of systemic candidiasis. Even though fungal burdens are comparable between the *hat1Δ/Δ* mutant and the wild-type 7 days post infection, the mutant is strongly attenuated in killing the host. Since kidney failure is the primary cause of death in this particular mouse infection model [64,65] we determined the degree of kidney injury or function in infected mice by measuring serum urea levels. As expected due to the lower fungal

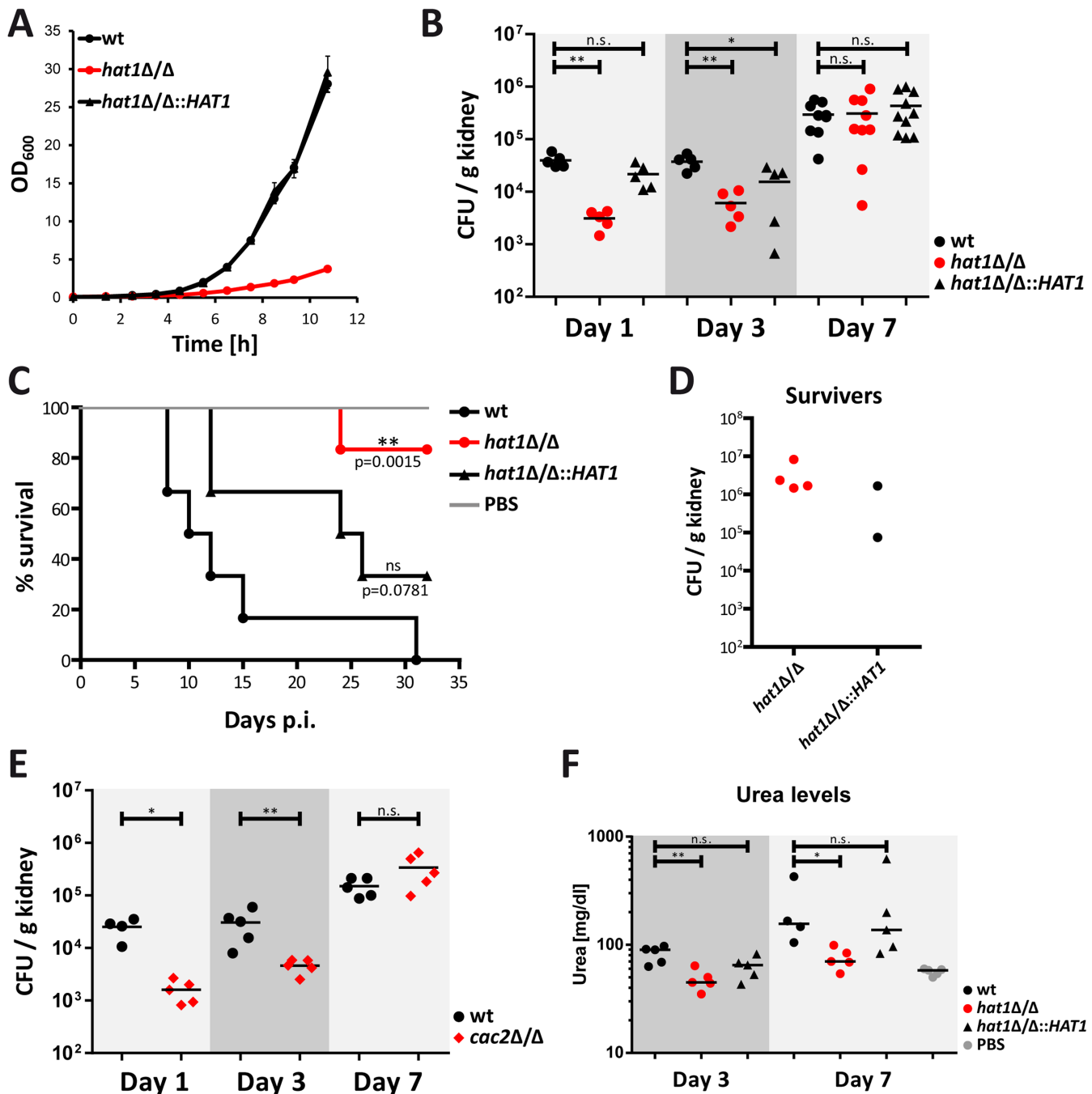


**Fig 9. Cells lacking Hat1 show reduced virulence but persist in mouse kidneys.** (A) Reduced growth rate of the *hat1Δ/Δ* strain was determined by measuring the OD<sub>600</sub> of cells growing in YPD at 30°C. (B) Cells lacking Hat1 are not cleared efficiently from kidneys. At the indicated time points, fungal burdens in kidneys of mice infected with *C. albicans* strains were determined and expressed as CFUs per gram kidney. Groups of 5–10 mice were analyzed at each time point and statistical significance was determined using the non-parametric Mann-Whitney-test. n.s.: not significant, \*P<0.05 and \*\*P<0.01 relative to the corresponding wild-type. (C) *hat1Δ/Δ* cells are defective in killing the host. Survival of mice infected with the indicated strains was monitored over 32 days post infection (p.i.). The data are presented as Kaplan-Meier survival curves. Groups of 6 mice were infected per *C. albicans* strain. Statistical significance was determined using the Log-rank test. ns: not significant; (D) Fungal burdens in kidneys of surviving mice from panel C were determined and expressed as CFUs per gram organ. One mouse infected with the *hat1Δ/Δ* strain was able to clear *Candida*. (E) The *cac2Δ/Δ* strain is not cleared efficiently from kidneys. Experiment was performed as described in (B). Groups of 4–5 mice were analyzed at each time point. (F) Infection with *hat1Δ/Δ* cells causes reduced kidney damage. Urea levels were determined in sera of infected mice at day 3 and 7 post infection. n.s.: not significant, \*P<0.05, \*\*P<0.01 relative to the wild-type (Student's t-test).

doi:10.1371/journal.ppat.1005218.g009

burden, mice infected with the *hat1Δ/Δ* mutant showed reduced urea levels at day 3. The reintegrant again yielded in an intermediate phenotype (Fig 9F). However, at day 7 lack of Hat1 still yielded in lower urea levels when compared to the wild-type (Fig 9F). Thus, lack of Hat1 seems to cause reduced kidney injury even at comparable fungal burdens. In summary, our data suggest that the *hat1Δ/Δ* strain is able to compensate its *in vitro* growth defect *in vivo* and persist in the host. However, cells lacking Hat1 are severely compromised in killing the host.

## Discussion

### Regulation of oxidative stress genes via chromatin assembly

In this work, we provide compelling evidence for a novel function of the eukaryotic histone acetyltransferase Hat1 in the pathogenic fungus *C. albicans*. Hat1 is required for regulating oxidative stress response, antifungal drug tolerance as well as virulence. We show that Hat1 functions in distinct chromatin assembly pathways acting in concert with well-known histone chaperones CAF-1 and HIR. Hence, in addition to an evolutionary conserved role of Hat1 in DNA damage repair [10,41,66,67] our data demonstrate a novel function for Hat1 in regulating the response to oxidative stress and azole treatment. Furthermore, certain resistance phenotypes as well as gene sets misregulated upon loss of Hat1 are also affected by distinct histone chaperones operating in independent chromatin assembly pathways. Thus, our data suggest that the Hat1 histone acetyltransferase has a central function in mediating the flux of histones necessary for nucleosome remodeling in *C. albicans* thereby affecting various cellular processes, including fungal virulence and persistence in the host.

Interestingly, the function in the regulation of the ROS response seems restricted to *C. albicans* and related fungal CTG clade members. This has not been reported in other organisms so far. This function of Hat1 might have developed only recently, providing an explanation why this is only observed in a small number of fungal species. Of note, Rtt109 from non-pathogenic *S. cerevisiae* negatively regulates catalase expression in response to H<sub>2</sub>O<sub>2</sub> together with Asf1 via histone deposition, whereby lack of Asf1 or Rtt109 increases RNAPII recruitment [33]. Likewise, we detect increased RNAPII levels at several oxidative stress genes immediately after induction in the *hat1Δ/Δ* mutant (Fig 6). While the *S. cerevisiae rtt109Δ* mutant displays slightly increased H<sub>2</sub>O<sub>2</sub> resistance (S5 Fig), the *C. albicans RTT109* deletion fails to effect catalase induction or peroxide resistance (S1C and S2E Figs). Thus, it is very tempting to speculate that Hat1 and Rtt109 are involved in the regulation of distinct gene sets in different species. Noteworthy, Asf1 interacts with Hat1 in *S. cerevisiae* [68]. Whether Hat1 regulates oxidative stress response in *C. albicans* also via Asf1 remains unclear, since Asf1 is an essential gene in *C. albicans*. Asf1 is also essential in *S. pombe* and *Drosophila melanogaster* [69,70], implying increased functional redundancy in histone chaperone functions in *S. cerevisiae* when compared to *C. albicans* and other species.

Of particular interest is that Spt6 negatively regulates catalase expression in *S. cerevisiae* [33]. The observed H<sub>2</sub>O<sub>2</sub> resistance phenotype of the *C. albicans spt6Δ/Δ* mutant might indicate conservation of this function in both species. Although interesting, further experiments are needed to determine the molecular mechanism(s) of oxidative stress regulation in cells lacking Spt6.

We show here that genetic removal *HAT1* accelerates the induction kinetics of oxidative stress genes, including catalase as well as other genes encoding glutathione-utilizing enzymes. However, the lack of catalase in a *hat1Δ/Δ* background does not lower the H<sub>2</sub>O<sub>2</sub> sensitivity to the level of the *cat1Δ/Δ* single knock-out (Fig 7C). On the other hand, the absence of Hat1 combined with defects in glutathione biosynthesis does not significantly increase H<sub>2</sub>O<sub>2</sub> tolerance (Fig 7D). Therefore, the H<sub>2</sub>O<sub>2</sub> resistance phenotype of the *hat1Δ/Δ* deletion strain is likely

to be due to the upregulation of glutathione-utilizing enzymes, although a contribution of Cat1 cannot be fully excluded at this point.

## Repression of genes via distinct chromatin assembly pathways

Interestingly, novel functions for the CAF-1 and HIR histone chaperone complexes in the regulation of white-opaque switching were reported for *C. albicans* [71]. The CAF-1 and HIR chaperone complexes are essential for histone deposition via distinct pathways. While the HIR complex functions in replication-independent chromatin assembly, CAF-1 is thought to mediate replication-coupled histone deposition [21,44,72].

To the best of our knowledge, no reports exist suggesting a role for Hat1 acting through the HIR complex to modulate antifungal drug resistance in any other eukaryote. Of note, this Hat1 function may have been conserved in some fungal species, since elevated azole tolerance is at least observed in *S. pombe* lacking the Hat1 orthologue. Of note, *HAT1* is indeed repressed in *C. albicans* cells treated with itraconazole, implying a function for Hat1 in the regulation of azole susceptibility [73]. Furthermore, our RNA-Seq data demonstrate a downregulation of ergosterol biosynthesis genes in the *hat1Δ/Δ* strain, including *ERG3* whose lack confers pronounced azole resistance [74]. Thus, a similar mechanism may explain the reduced susceptibility of *hat1Δ/Δ* and *hir1Δ/Δ* strains. Another mechanism mediating the increased azole tolerance could be the upregulation of multidrug transporters [75,76]. The two major ATP-binding cassette transporters responsible for azole resistance in *C. albicans* are Cdr1 and Cdr2 [77–80]. Whereas only *CDR2* was slightly upregulated in *hat1Δ/Δ* cells, the major facilitator superfamily transporter Mdr1, which is also induced upon oxidative stress and confers azole resistance [77,81], is significantly upregulated in the *hat1Δ/Δ* mutant upon treatment with H<sub>2</sub>O<sub>2</sub> (S1 Table). However, the exact mechanism by which Hat1 and Hir1 regulate azole tolerance remains to be determined in future studies.

Although, the CAF-1 complex can assemble histones in a replication-coupled manner, it can also influence the rate of replication-independent histone incorporation and transcription [22,82,83]. Therefore, NuB4 and CAF-1 might act in concert to regulate specific target genes such as oxidative stress response sets in *C. albicans*. We propose that they do so by facilitating histone incorporation concomitant with transcription, thereby increasing the histone density. Indeed, we observe a large overlap in differentially expressed gene sets in *hat1Δ/Δ* and the *cac2Δ/Δ* mutants, the latter lacking a subunit of CAF-1 (Fig 4D and 4E). Unfortunately, we were not able to obtain a *hat1Δ/Δ cac2Δ/Δ* double deletion strain for epistasis analysis. Thus, we cannot completely rule out the possibility that Hat1 and Cac2 regulate H<sub>2</sub>O<sub>2</sub> resistance independently. One explanation for a possible synthetic lethality of *hat1Δ/Δ cac2Δ/Δ* double mutants may be that both are associated with essential DNA replication [21,84,85].

The genome-wide transcriptional RNA-Seq profiling of logarithmically growing *hat1Δ/Δ* cells mainly revealed upregulation of genes, suggesting repressive functions of Hat1. Notably, distinct GO terms are enriched in the *hat1Δ/Δ* mutant alone or in overlaps with other mutants. These data suggest specific functions for Hat1 in different processes, including DNA damage repair, arginine biosynthesis and mitochondrial degradation (Fig 5). Interestingly, Rtt109 inhibits arginine biosynthesis genes in *S. cerevisiae* together with Asf1 under repressing conditions [86]. By contrast, this gene set is derepressed in *C. albicans hat1Δ/Δ* and *cac2Δ/Δ*, but not in *rtt109Δ/Δ* cells (Fig 5B and 5C). Thus, we believe that Hat1/Cac2 have taken over this function from Rtt109 in *C. albicans*. Interestingly enough, mitochondrial dysfunction has been linked to azole and oxidative stress sensitivity in *C. albicans*, as well as in other fungal species [87–89]. However, depletion of Fzo1, which is involved in mitochondrial fusion, and Goa1, a protein localizing to mitochondria upon oxidant treatment [87,88], decreases azole and

oxidative stress tolerance. Thus, although genes involved in mitochondrion degradation are upregulated in *hat1Δ/Δ* cells, the loss of mitochondrial function is unlikely to explain the increase in stress resistance.

Interestingly, upon H<sub>2</sub>O<sub>2</sub> treatment we observed increased expression of genes involved in ncRNA/rRNA processing specifically in the *hat1Δ/Δ* mutant (Fig 5E and 5F). However, this group of genes is repressed in the wild-type upon H<sub>2</sub>O<sub>2</sub> stress. Only 4 out of a total of 119 *hat1Δ/Δ* upregulated genes in this group were less than 2-fold repressed in the wild-type. Thus, lack of Hat1 seems to cause a defect in repression of genes involved in ncRNA/rRNA processing and ribosome biogenesis. Although a faster induction kinetics of genes connected to H<sub>2</sub>O<sub>2</sub> resistance occurs upon loss of Hat1 (Fig 6A and 6D), many oxidative stress-regulated genes appear not significantly modulated in the RNA-Seq dataset making GO term enrichment for this group futile. A possible explanation is that many stress conditions in fungi, including oxidative stress or osmostress, follow a stress-specific and often transient regulation [90], which may result in difficulties choosing the correct timing for collecting data points in *hat1Δ/Δ* and wild-type cells. Nevertheless, we speculate that the Hat1-mediated oxidative stress regulation may relate to host infection conditions, where severe oxidative stress is a major immune defense during phagocytosis of fungal pathogens [26,91].

### Inactivation of Hat1 compromises virulence in *C. albicans*

Although infection of macrophages or neutrophils by the *hat1Δ/Δ* mutant strongly reduces total ROS accumulation, we observed faster accumulation of ROS in the beginning of the interaction (Fig 8B and S3A Fig). Differences in ROS production cannot be simply explained by the pseudohyphal morphology of cells lacking Hat1, since the *rtt109Δ/Δ* strain has the same morphological defect [30] yet does not show any differences in ROS accumulation (Fig 8B). Thus, it may specifically result from Hat1-mediated gene regulation and from upregulated factors triggering ROS production. Interestingly enough, a mouse model of virulence yields compelling data showing that *hat1Δ/Δ* cells display strongly attenuated virulence. Of note, infected mice show significantly reduced organ burdens of *hat1Δ/Δ* cells immediately after infection, but reach comparable levels of fungal burdens between day 3 and day 7 post infection (Fig 9B). This implies a faster growth *in vivo*, which may be explained by the reduced susceptibility to neutrophil-mediated killing, essentially providing a “fitness” advantage of *hat1Δ/Δ* *in vivo*. Moreover, cells lacking Hat1 cause less damage to host organs and therefore enable better mouse survival. Reduced urea levels in sera of infected mice support this notion (Fig 9F). In line with this hypothesis is also the fact that *hat1Δ/Δ* cells degrade ROS more efficiently, protecting the *hat1Δ/Δ* mutant from clearance by the immune surveillance. This may also result in reduced tissue damage, since reactive oxygen species originating from innate immune response are harming both the pathogen and the host due to increasing inflammation [92,93]. Indeed, a downmodulation of the inflammatory immune response can be beneficial for the host during invasive *Candida albicans* infections [65,94]. Finally, ROS is also known as a signaling molecule during infections and reduced levels upon challenge with the *hat1Δ/Δ* mutant might impact the immune response [95].

Furthermore, compelling evidence exists suggesting that the *hat1Δ/Δ* virulence phenotype is not just due to its role in DNA damage repair. Deletion of *RAD52* or *RTT109* also causes pseudohyphal cell morphology and strong virulence defects in mouse models of systemic candidiasis [28,30,96]. However, the *rtt109Δ/Δ* mutant is efficiently cleared from kidneys of infected mice 3 days post infection [30]. Likewise, kidney fungal burdens of *rad52Δ/Δ* cells decline over 3 days post infection even with an inoculum concentration ten times higher than in our setup [28]. By sharp contrast, the *hat1Δ/Δ* fungal burdens in kidneys increase, reaching wild-type

levels 7 days post infection. Nonetheless, despite increased growth *in vivo*, removal of Hat1 renders cells unable to kill the host efficiently over 32 days, consistent with a persistent but avirulent invasive infection (Fig 9C).

## Evolution of specialized functions for chromatin assembly pathways in *C. albicans*

Our data unequivocally show that loss of Hat1, Cac2 and Hir1 can be beneficial for *C. albicans* in our experimental setup. However, the inability to efficiently repress genes under stress conditions might also be detrimental for the organism. Furthermore, loss of Hat1 and Cac2 also impairs DNA damage repair and thus promotes genome instability [10,71]. Thus, the resulting fitness loss due to the absence of these factors might be disadvantageous in the long run, despite a gain in oxidative resistance. Further experiments are required to identify additional factors functioning together with NuB4/CAF-1 and NuB4/HIR in the regulation of oxidative stress resistance or azole tolerance. This might also lead to the discovery of potential antifungal targets, which could be used to render cells more sensitive to ROS or azoles. Importantly, the data from the mouse model imply that inhibitors of HATs could have beneficial effects in clinical therapeutic settings but pose the risk of promoting persistent or latent infections.

Interestingly, we don't observe comparable resistance phenotypes upon genetic removal of Hat1 in *S. cerevisiae*, *C. glabrata* and at least for the oxidative stress resistance also in *S. pombe* (Fig 3). Thus, in *C. albicans*, the NuB4 and CAF-1 complexes might have gained functions during coevolution with the human host, which appears restricted to the CTG clade. Hence, deletion of *HAT1* in *C. glabrata*, the second-most prevalent human fungal pathogen [24], does not result in similar phenotypes. Nonetheless, our results clearly demonstrate substantial differences in the functions of even highly conserved chromatin modification mechanisms between *C. albicans* and other fungi. Therefore, results obtained from classical model systems such as baker's yeast often cannot simply be transferred to pathogenic fungi.

The regulation of virulence-associated traits by chromatin modification has been reported for several pathogens and it is now generally accepted that the chromatin status affects virulence [97,98]. Moreover, several reports suggest that chromatin modifiers are involved in the regulation of fungal virulence factors including antifungal drug tolerance [97,99–102]. Hence, modulation of chromatin function or chromatin-modifying pathways including nucleosome remodeling may be a common strategy during coevolution of microbial pathogens with the host to promote immune evasion.

## Materials and Methods

### Ethics statement

All animal experiments were evaluated by the ethics committee of the Medical University of Vienna and approved by the Federal Ministry for Science and Research, Vienna, Austria (GZ: BMWF- 68.20n5/231-II/3b/2011) adhering to European legislation for animal experimentation.

### Media, chemicals and growth conditions

Rich medium (YPD) and synthetic complete medium (SC) were prepared as previously described [103]. Minimal medium contained 8.38 g/l yeast nitrogen base (BD Biosciences), 6.25 g/l ammonium sulfate (Sigma Aldrich) and 2 g/l glucose (Sigma Aldrich). Fungal strains were routinely grown on YPD plates at 30°C. Hydrogen peroxide, tert-butyl hydroperoxide, Calcofluor White, Congo Red, cadmium chloride, sodium chloride, luminol and HRP Type VI

were obtained from Sigma Aldrich. Voriconazole, Itraconazole and Amphotericin B were purchased from Discovery Fine Chemicals Ltd. DMEM and RPMI media were purchased from PAA.

## Plasmid and strain construction and genomic verification

A list of fungal strains, plasmids and primers used in this study is shown in Tables A, B and C in [S1 Text](#), respectively. All *C. albicans* strains constructed in this work were derived from the clinical isolate SC5314 [104]. For deletion of *HAT1* in *C. parapsilosis* the clinical isolate GA1 was used [105]. Disruption of *HAT1* in *C. tropicalis* was done in the clinical isolate AKH2249. Deletion of *CAC2* and *HIR1* was done using a modified version of the SAT1 flipper method [106]. Briefly, the marker cassette was amplified using the pSFS3b plasmid and primers containing some 80bp homologous region to replace the whole coding sequence of the corresponding gene [10]. For deletion of *RTT106* two primer pairs were used to add the homologous regions in two sequential PCR steps. For deletion of *CAT1*, YEp352-SAT1-*CAT1*urdr was constructed by *in vivo* cloning in *S. cerevisiae* exactly as described previously [107]. Plasmids for deletion of *GCS1*, *GSH2*, *C. tropicalis HAT1* and *C. parapsilosis HAT1* were constructed by fusing ~500bp fragments upstream and downstream of the corresponding gene with a FRT-FLP-NAT1-FRT cassette derived from pSFS3b [10] and a fragment containing an ampicillin resistance cassette and an *E. coli* replication origin derived from YEp352 [108] via *in vivo* recombination in *E. coli* EL350 as described in [109]. Due to low transformation efficiency for *C. parapsilosis* and *C. tropicalis* a second set of deletion vectors was constructed in the same way to obtain the homozygous knock-outs. These vectors contained 300–350bp of the beginning and the end of the corresponding CDS for homologous recombination to avoid integration at the deleted allele. For construction of the *CAC2* reintegration plasmid the coding sequence plus ~500 up- and downstream was amplified and cloned into pSFS3b via *KpnI* and *ApaI*. Transformation of *C. albicans* was done via electroporation [106]. Correct integration of the deletion cassette and loss of the corresponding gene were confirmed by colony PCR.

Colony PCR assays were used to verify correct genomic integration of deletion constructs. Briefly, a colony was resuspended in 25  $\mu$ l H<sub>2</sub>O in a PCR tube and incubated at 95°C for 10 minutes. Cell debris was spun down briefly and 5  $\mu$ l of the supernatant was used as template for the PCR, which was performed using the DreamTaq Green DNA Polymerase (Thermo Scientific) according to the manufacturer's instructions.

## Spot dilution and liquid survival/growth inhibition assays

Spot dilution assays were performed as described previously [10]. For determination of H<sub>2</sub>O<sub>2</sub> survival logarithmically growing cells in YPD were treated with the indicated concentrations of hydrogen peroxide for 2 hours at 30°C. Before and after treatment cells were diluted and plated on YPD plates. For the H<sub>2</sub>O<sub>2</sub> survival shown in [Fig 7D](#) cells were grown overnight in minimal medium, diluted to OD<sub>600</sub> of 0.2 and further incubated at 30°C for 5 hours. Cells were harvested by centrifugation at 1500 g for 3 minutes, resuspended at an OD<sub>600</sub> of 0.5 and treated with 0.5 mM H<sub>2</sub>O<sub>2</sub> for 2 hours. Before and after treatment cells were diluted and plated on YPD plates containing 1 mM glutathione. Colonies were counted after 3 days incubation at 30°C and viability was determined relative to the samples plated before H<sub>2</sub>O<sub>2</sub> addition. To quantify growth inhibition by azole treatment cells were grown to logarithmic phase in SC medium at 30°C. Cultures were diluted to an OD<sub>600</sub> of 0.01 in SC medium with or without voriconazole at the indicated concentrations. OD<sub>600</sub> was determined after growth at 30°C for 18–24 hours. For *C. parapsilosis* cultures were incubated for 41 hours due to the slow growth rate of the *hat1* $\Delta/\Delta$  mutant. Growth inhibition was calculated relative to untreated controls.

## RNA isolation, RT-qPCR analysis and RNA-seq

Cells were grown in YPD overnight to an  $OD_{600}$  of 1 at 30°C. For hydrogen peroxide treatment 1.6 mM  $H_2O_2$  was added to the culture for the indicated period of time. RNA isolation and qPCR analysis was done as described previously [10]. For RT-qPCRs shown in Fig 8A, *RIP1* was used as reference gene [99]. All other RT-qPCRs were normalized to *PAT1* [110].

After RNA isolation, 10  $\mu$ g total RNA were treated with DNase I (Thermo Scientific) and purified using the RNeasy MinElute Cleanup Kit (Qiagen). 5  $\mu$ g DNase treated RNA were used for rRNA depletion with the RiboMinus Eukaryote System v2 (Life Technologies, Carlsbad, CA). rRNA depleted samples were fragmented using the NEBNext Magnesium RNA Fragmentation Module (New England Biolabs) and purified with the RNeasy MinElute Cleanup Kit (Qiagen). SuperScript III reverse transcriptase (Life Technologies, Carlsbad, CA) was used for first strand synthesis. Priming was done with 3  $\mu$ g random hexamers (Life Technologies). Samples were purified using Mini Quick Spin Columns (Roche) and second strand synthesis was done with the NEBNext mRNA Second Strand Synthesis Module (New England Biolabs). Final purification of double stranded cDNA was done with the MinElute PCR Purification Kit (Qiagen). Samples were further processed and sequenced on a HiSeq 2000 instrument (Illumina) at the Next Generation Sequencing Facility (CSF NGS unit, <http://www.csf.ac.at>) of the Campus Vienna Biocenter. For both conditions five biological replicates for the wild-type as well as the *hat1* $\Delta/\Delta$  strain and three biological replicates for the *cac2* $\Delta/\Delta$  as well as the *rtt109* $\Delta/\Delta$  mutants were sequenced.

Reads were mapped onto the Assembly 21 of the *C. albicans* genome (<http://www.candidagenome.org>) using NextGenMap [111]. Read counts were determined with HTSeq using the union mode [112] and a reference annotation (*C\_albicans\_SC5314\_version\_A21-s02-m07-r10*; <http://www.candidagenome.org>). The annotation of the coding sequence assembly was used as transcript coordinates. For short non-coding RNAs (tRNAs, snRNAs, snoRNAs and ncRNAs) 20bp up- and downstream of their chromosomal coordinates were added before mapping [113]. Differential expression analysis was done with edgeR [114]. Benjamini-Hochberg adjusted p-values were used to determine differentially regulated genes [115]. Venn diagrams were created using Venny 1.0 [116]. Gene ontology (GO) term enrichment was determined using the GO Term finder (<http://www.candidagenome.org>). Overlapping GO terms were merged manually.

## Chromatin immunoprecipitation

Chromatin immunoprecipitation was performed as described previously [113]. One mg whole cell extract was used per ChIP. For determination of histone density an antibody against the C-terminus of histone H3 was used (ab1791, Abcam). Detection of RNAPII was done with an antibody against the C-terminal domain (05–592, clone 8WG16, Millipore). To analyze the *CAT1* promoter region primers amplifying a fragment ranging from -315 to -163 with respect to the start codon were used. To determine enrichment within the *CAT1*, *GPX1* and *GST1* genes primers within these coding regions were used. Signals were normalized to an intergenic region on chromosome R.

## Enzymatic assays, immunoblotting and mass spectrometric analysis

To quantify catalase activity, cells were grown overnight to an  $OD_{600}$  of 1 at 30°C. For hydrogen peroxide treatment 1.6 mM  $H_2O_2$  was added to the culture for one hour. Before and after treatment 20 ml culture were harvested at 1500 g for 3 min at 4°C and washed once with 20 ml cold  $H_2O$ . Pellets were resuspended in 250  $\mu$ l lysis buffer [50 mM Tris-HCl pH 7.5; 10% glycerol, complete protease inhibitor cocktail (Roche)] and an equal volume of glass beads (425–

600mm, Sigma Aldrich) was added. Cells were lysed by shaking 5 times at  $6\text{ m s}^{-1}$  for 30 s on a FastPrep instrument (MP Biomedicals). Extracts were cleared by centrifugation at 14000 g for 5 min at 4°C. Protein concentration in the extracts was determined by measuring absorption at 280 nm. For catalase activity measurement 5–40  $\mu\text{l}$  whole cell extract were added to 3 ml of catalase assay buffer [384 mM  $\text{Na}_3\text{PO}_4$ ; 0.015 mM Triton X-100 (Sigma Aldrich); 11.4 mM  $\text{H}_2\text{O}_2$ ] and degradation of  $\text{H}_2\text{O}_2$  was determined by measuring absorbance at 240 nm for up to 2 min. Catalase activity was calculated in  $\mu\text{M H}_2\text{O}_2$  per minute per mg of whole cell extract as described previously [117] ( $\epsilon = 43.6$ ).

Glutathione peroxidase assays were performed as previously described [118] using some modifications. The lysis buffer used contained 50 mM Tris-HCl, pH 7.5, 150 mM NaCl, 0.5 g/100 ml Nonidet P-40 and complete protease inhibitor cocktail (Roche, Basel, Switzerland). Cell lysis was performed as described for the catalase assay. 10–50  $\mu\text{l}$  cleared whole cell extract was used for the assay exactly as described in [118].

Sample preparation and western blot analysis were essentially carried out as described previously [119]. A MOI of 5:1 (fungi to macrophages) was used and samples were harvested after 30 min of interaction. Activated NADPH oxidase was detected using an antibody against the phosphorylated p40phox subunit (Cell Signaling 4311). A panERK antibody (BD 610123) was used as loading control.

Whole cell extracts for mass spectrometric analysis were prepared by lysing logarithmically growing cells in MS lysis buffer [10 mM Tris-HCl pH 7.5; complete protease inhibitor cocktail (Roche)] with a French press. Extracts were lyophilized, resuspended in 2 M urea and used for trypsin digestion followed by liquid chromatography—tandem mass spectrometry analysis on a LTQ Orbitrap Velos system (Thermo Scientific).

## Mouse strains and immune cells (bone marrow-derived macrophages and neutrophils)

For all experiments, 7–10 week old C57BL/6 wild-type mice were used. Isolation and cultivation of primary bone marrow-derived macrophages was done as described previously [26]. Isolation of bone marrow neutrophils and subsequent *C. albicans* survival assays were performed as described earlier [65]. A MOI of 1:10 (fungi to neutrophils) was used, and cells were harvested after a 1-hour interaction.

Mouse infections were carried out through lateral tail vein injections as described previously with some minor modifications [65]. Briefly, *C. albicans* strains were grown overnight to an  $\text{OD}_{600}$  of around 1, washed twice and finally resuspended in PBS. For infection,  $1 \times 10^5$  *Candida* cells per 21 g mouse body weight were injected via the lateral tail vein. For survival experiments, mice were monitored for 32 days. Analysis of fungal burdens in the kidneys at day 1, 3 and 7 post infection, as well as determination of serum urea levels was done exactly as described previously [65]. Statistical analysis was carried out using the Prism software (Graphpad Software Inc.).

## ROS and phagocytosis assays

ROS assays were done exactly as described previously [26]. The multiplicity of infection (MOI) for all ROS assays was 5:1 (fungi to immune cells). Phagocytosis assays were performed essentially as described with some modifications [119]. *C. albicans* cells were grown overnight to an  $\text{OD}_{600}$  of around 1, washed twice in PBS and stained with  $10\text{ mg ml}^{-1}$  Alexa Fluor 488 (Life Technologies) in 100 mM HEPES buffer (pH 7.5) for 60 min at 30°C shaking in the dark. After staining cells were washed 3 times, resuspended in HEPES buffer and used for interaction with BMDMs. Stained *Candida* cells were added to macrophages and incubated for 45 min at 37°C

and 5% CO<sub>2</sub>. Control reactions were kept on ice during the whole procedure. A MOI of 2:1 (fungi to macrophages) was used. Phagocytosis was terminated by chilling on ice. Plates remained on ice during subsequent detaching and fixation in 1% formaldehyde. Extracellular fluorescent *C. albicans* cells were quenched by addition of 0.4% trypan blue. Samples were subject to flow cytometry analysis with FL1-H on a FACSCalibur instrument (BD Biosciences).

## Supporting Information

**S1 Fig. Loss of Hat1 causes oxidative stress resistance.** (A) Resistance to other stress conditions is unchanged in *hat1Δ/Δ* cells. CFW: Calcofluor White; CR: Congo Red; AmB: Amphotericin B; (B) Loss of Hat1 increases resistance to diamide. (C) Lack of proteins involved in DNA damage repair does not increase resistance to H<sub>2</sub>O<sub>2</sub>. (D) Deletion of *CAC2* causes increased tBOOH resistance. Loss of *Rtt109* does not affect tBOOH resistance. (A-D) Fivefold serial dilutions of the indicated strains were spotted on agar plates containing the indicated substances and pictures were taken after incubation at 30°C for 3 days. (TIF)

**S2 Fig. Deletion of *HAT1* causes upregulation of tRNAs and *CAT1*.** (A) Treatment with 1.6 mM H<sub>2</sub>O<sub>2</sub> does not kill *C. albicans*. Cells of the indicated strains were treated for 1 hour, plated and colonies counted after 3 days of incubation on YPD plates at 30°C to determine viability. Data are shown as mean + SD from two independent experiments. (B) H<sub>2</sub>O<sub>2</sub> repressed ncRNAs are upregulated in the *hat1Δ/Δ* mutant upon peroxide treatment. Each dot corresponds to one ncRNA. The fold change in RNA expression between H<sub>2</sub>O<sub>2</sub> treated wild-type and *hat1Δ/Δ* strains (y-axis) is plotted against the fold change between the wild-type without and with treatment (x-axis). Differentially expressed ncRNAs (fold change ≥ 2 and p-value < 0.05) in the *hat1Δ/Δ* mutant are depicted in red. logFC: log<sub>2</sub> fold change; (C) GO terms enriched among 1.5-fold upregulated proteins in logarithmically growing *hat1Δ/Δ* cells are shown. Expression levels were determined by mass spectrometric analysis as described in the Materials and Methods section. Fold changes relative to the wild-type were calculated using the spectra counts. The corresponding p-values for the enrichment (empty bars) and the percentage of proteins changed within the GO group (filled bars) are presented. The absolute number of regulated proteins within a GO group is presented in brackets. (D) Derepression of *CAT1* in logarithmically growing cells was detected by RT-qPCR. Transcript levels were normalized to the expression level of the reference gene (RG) *PAT1*. Data are shown as mean + SD from 3 independent experiments. (E) Increased *CAT1* induction levels were only observed for *hat1Δ/Δ* and *cac2Δ/Δ* cells, but not for cells lacking *Rtt109*. Cells were treated with 1.6 mM H<sub>2</sub>O<sub>2</sub> for 30 min. Transcript levels were normalized to the expression level of *PAT1*. Data are shown as mean + SD from 3 independent experiments. (C-D) \*P < 0.05, \*\*P < 0.01, \*\*\*P < 0.001 relative to the corresponding control (Student's t-test). (TIF)

**S3 Fig. Loss of Hat1 causes reduced ROS accumulation upon interaction with neutrophils.** (A) ROS levels were determined by measuring luminol-dependent chemiluminescence [relative luciferase units (RLU) min<sup>-1</sup> per 1000 immune cells] in 2.5 min intervals during interaction of the indicated *C. albicans* strains with murine bone marrow neutrophils. One representative experiment is shown. Data were reproduced in two independent experiments. (B) Cells lacking Hat1 are phagocytosed at the same rate as the wild-type. Phagocytosis was quantified by measuring the fraction of BMDMs containing labelled *C. albicans* cells upon 45 min interaction at 37°C (5% CO<sub>2</sub>) by FACS. Control reactions were kept at 4°C. BMDMs without *C. albicans* were also included (Mphs only). One representative experiment is shown. Data were

reproduced in two independent experiments. FL1-H: FITC intensity (C) NADPH oxidase is activated to the same extent upon infection with wild-type or *hat1Δ/Δ* cells. Activation of the NADPH oxidase in BMDMs upon 30 min interaction was determined by detection of the phosphorylated p40phox subunit. ERK levels served as loading control. An uninfected control was included (wo Ca). The asterisk marks a cross reaction. One representative experiment is shown. Data were reproduced in two independent experiments.

(TIF)

**S4 Fig. Reduced body weight loss upon infection with *hat1Δ/Δ* or *cac2Δ/Δ* cells.** (A and B)

Body weight of mice infected with the indicated *Candida* strains was determined daily until day 6 post infection (p.i.). Significance was determined relative to wild-type infected mice using Two-way ANOVA. \*\*\*P<0.001.

(TIF)

**S5 Fig. Deletion of *RTT109* in *S. cerevisiae* increases H<sub>2</sub>O<sub>2</sub> resistance.** Fivefold serial dilutions of the indicated strains were spotted on agar plates containing the indicated substances and pictures were taken after incubation at 30°C for 3 days.

(TIF)

**S1 Table. RNA-Seq results.**

(XLSX)

**S1 Text. Fungal strains, plasmids and oligonucleotides used in this study.** Table A. Fungal strains used in this study. Table B. Plasmids used in this study. Table C. Oligonucleotides used in this study.

(DOCX)

## Acknowledgments

We thank all laboratory members for helpful discussions. We are grateful to Joseph Bliss for providing the *C. albicans* strains JMB220 and JMB31, Anthony Annunziato for sending the *S. pombe* strains 975 and LBP6, Attila Gácsér for the gift of the *C. parapsilosis* strain GA1, and Birgit Willinger for providing the clinical isolate *C. tropicalis* strain AKH2249. *C. albicans* sequence data were obtained from the Stanford Genome Center (<http://www.candidagenome.org>).

## Author Contributions

Conceived and designed the experiments: MT FZ KK NC. Performed the experiments: MT FZ SJ AP IEF JM. Analyzed the data: MT FJS KK. Contributed reagents/materials/analysis tools: NC AvH. Wrote the paper: MT KK.

## References

1. Luger K, Mäder AW, Richmond RK, Sargent DF, Richmond TJ (1997) Crystal structure of the nucleosome core particle at 2.8 Å resolution. *Nature* 389: 251–260. PMID: [9305837](#)
2. Chen CC, Carson JJ, Feser J, Tamburini B, Zabaronick S, et al. (2008) Acetylated lysine 56 on histone H3 drives chromatin assembly after repair and signals for the completion of repair. *Cell* 134: 231–243. doi: [10.1016/j.cell.2008.06.035](#) PMID: [18662539](#)
3. Franco AA, Lam WM, Burgers PM, Kaufman PD (2005) Histone deposition protein Asf1 maintains DNA replisome integrity and interacts with replication factor C. *Genes Dev* 19: 1365–1375. PMID: [15901673](#)
4. Kaplan CD, Laprade L, Winston F (2003) Transcription elongation factors repress transcription initiation from cryptic sites. *Science* 301: 1096–1099. PMID: [12934008](#)

5. Saunders A, Werner J, Andrusis ED, Nakayama T, Hirose S, et al. (2003) Tracking FACT and the RNA polymerase II elongation complex through chromatin *in vivo*. *Science* 301: 1094–1096. PMID: [12934007](#)
6. Schwabish MA, Struhl K (2004) Evidence for eviction and rapid deposition of histones upon transcriptional elongation by RNA polymerase II. *Mol Cell Biol* 24: 10111–10117. PMID: [15542822](#)
7. Tsukuda T, Fleming AB, Nickoloff JA, Osley MA (2005) Chromatin remodelling at a DNA double-strand break site in *Saccharomyces cerevisiae*. *Nature* 438: 379–383. PMID: [16292314](#)
8. Parthun MR (2012) Histone acetyltransferase 1: More than just an enzyme? *Biochim Biophys Acta* 1819: 256–263. doi: [10.1016/j.bbagr.2011.07.006](#) PMID: [21782045](#)
9. Parthun MR, Widom J, Gottschling DE (1996) The major cytoplasmic histone acetyltransferase in yeast: links to chromatin replication and histone metabolism. *Cell* 87: 85–94. PMID: [8858151](#)
10. Tscherner M, Stappler E, Hnisz D, Kuchler K (2012) The histone acetyltransferase Hat1 facilitates DNA damage repair and morphogenesis in *Candida albicans*. *Mol Microbiol* 86: 1197–1214. doi: [10.1111/mmi.12051](#) PMID: [23075292](#)
11. Parthun MR (2007) Hat1: the emerging cellular roles of a type B histone acetyltransferase. *Oncogene* 26: 5319–5328. PMID: [17694075](#)
12. Poveda A, Pamblanco M, Tafrov S, Tordera V, Sternglanz R, et al. (2004) Hif1 is a component of yeast histone acetyltransferase B, a complex mainly localized in the nucleus. *J Biol Chem* 279: 16033–16043. PMID: [14761951](#)
13. Driscoll R, Hudson A, Jackson SP (2007) Yeast Rtt109 promotes genome stability by acetylating histone H3 on lysine 56. *Science* 315: 649–652. PMID: [17272722](#)
14. Kelly TJ, Qin S, Gottschling DE, Parthun MR (2000) Type B histone acetyltransferase Hat1p participates in telomeric silencing. *Mol Cell Biol* 20: 7051–7058. PMID: [10982821](#)
15. Tong K, Keller T, Hoffman CS, Annunziato AT (2012) *Schizosaccharomyces pombe* Hat1 (Kat1) is associated with Mis16 and is required for telomeric silencing. *Eukaryot Cell* 11: 1095–1103. doi: [10.1128/EC.00123-12](#) PMID: [22771823](#)
16. Barman HK, Takami Y, Nishijima H, Shibahara K, Sanematsu F, et al. (2008) Histone acetyltransferase-1 regulates integrity of cytosolic histone H3–H4 containing complex. *Biochem Biophys Res Commun* 373: 624–630. doi: [10.1016/j.bbrc.2008.06.100](#) PMID: [18601901](#)
17. Campos EI, Fillingham J, Li G, Zheng H, Voigt P, et al. (2010) The program for processing newly synthesized histones H3.1 and H4. *Nat Struct Mol Biol* 17: 1343–1351. doi: [10.1038/nsmb.1911](#) PMID: [20953179](#)
18. Yang X, Li L, Liang J, Shi L, Yang J, et al. (2013) Histone acetyltransferase 1 promotes homologous recombination in DNA repair by facilitating histone turnover. *J Biol Chem* 288: 18271–18282. doi: [10.1074/jbc.M113.473199](#) PMID: [23653357](#)
19. Das C, Tyler JK, Churchill ME (2010) The histone shuffle: histone chaperones in an energetic dance. *Trends Biochem Sci* 35: 476–489. doi: [10.1016/j.tibs.2010.04.001](#) PMID: [20444609](#)
20. Huang S, Zhou H, Tarara J, Zhang Z (2007) A novel role for histone chaperones CAF-1 and Rtt106p in heterochromatin silencing. *EMBO J* 26: 2274–2283. PMID: [17410207](#)
21. Shibahara K, Stillman B (1999) Replication-dependent marking of DNA by PCNA facilitates CAF-1-coupled inheritance of chromatin. *Cell* 96: 575–585. PMID: [10052459](#)
22. Yu Z, Wu H, Chen H, Wang R, Liang X, et al. (2013) CAF-1 promotes Notch signaling through epigenetic control of target gene expression during *Drosophila* development. *Development* 140: 3635–3644. doi: [10.1242/dev.094599](#) PMID: [23942516](#)
23. Spector MS, Raff A, DeSilva H, Lee K, Osley MA (1997) Hir1p and Hir2p function as transcriptional corepressors to regulate histone gene transcription in the *Saccharomyces cerevisiae* cell cycle. *Mol Cell Biol* 17: 545–552. PMID: [9001207](#)
24. Pfaller MA, Diekema DJ (2007) Epidemiology of invasive candidiasis: a persistent public health problem. *Clin Microbiol Rev* 20: 133–163. PMID: [17223626](#)
25. Santos MA, Gomes AC, Santos MC, Carreto LC, Moura GR (2011) The genetic code of the fungal CTG clade. *C R Biol* 334: 607–611. doi: [10.1016/j.crv.2011.05.008](#) PMID: [21819941](#)
26. Frohner IE, Bourgeois C, Yatsyk K, Majer O, Kuchler K (2009) *Candida albicans* cell surface superoxide dismutases degrade host-derived reactive oxygen species to escape innate immune surveillance. *Mol Microbiol* 71: 240–252. doi: [10.1111/j.1365-2958.2008.06528.x](#) PMID: [19019164](#)
27. Pfaller MA, Andes D, Arendrup MC, Diekema DJ, Espinel-Ingroff A, et al. (2011) Clinical breakpoints for voriconazole and *Candida* spp. revisited: review of microbiologic, molecular, pharmacodynamic, and clinical data as they pertain to the development of species-specific interpretive criteria. *Diagn Microbiol Infect Dis* 70: 330–343. doi: [10.1016/j.diagmicrobio.2011.03.002](#) PMID: [21546199](#)

28. Chauhan N, Ciudad T, Rodriguez-Alejandre A, Larriba G, Calderone R, et al. (2005) Virulence and karyotype analyses of *rad52* mutants of *Candida albicans*: regeneration of a truncated chromosome of a reintegrant strain (*rad52/RAD52*) in the host. *Infect Immun* 73: 8069–8078. PMID: [16299301](#)
29. Hao B, Clancy CJ, Cheng S, Raman SB, Iczkowski KA, et al. (2009) *Candida albicans* *RFX2* encodes a DNA binding protein involved in DNA damage responses, morphogenesis, and virulence. *Eukaryot Cell* 8: 627–639. doi: [10.1128/EC.00246-08](#) PMID: [19252121](#)
30. Lopes da Rosa J, Boyartchuk VL, Zhu LJ, Kaufman PD (2010) Histone acetyltransferase Rtt109 is required for *Candida albicans* pathogenesis. *Proc Natl Acad Sci U S A* 107: 1594–1599. doi: [10.1073/pnas.0912427107](#) PMID: [20080646](#)
31. Tierney L, Linde J, Muller S, Brunke S, Molina JC, et al. (2012) An Interspecies Regulatory Network Inferred from Simultaneous RNA-seq of *Candida albicans* Invading Innate Immune Cells. *Front Microbiol* 3: 85. doi: [10.3389/fmicb.2012.00085](#) PMID: [22416242](#)
32. Fradin C, De Groot P, MacCallum D, Schaller M, Klis F, et al. (2005) Granulocytes govern the transcriptional response, morphology and proliferation of *Candida albicans* in human blood. *Mol Microbiol* 56: 397–415. PMID: [15813733](#)
33. Klopff E, Paskova L, Sole C, Mas G, Petryshyn A, et al. (2009) Cooperation between the INO80 complex and histone chaperones determines adaptation of stress gene transcription in the yeast *Saccharomyces cerevisiae*. *Mol Cell Biol* 29: 4994–5007. doi: [10.1128/MCB.01858-08](#) PMID: [19620280](#)
34. Adkins MW, Howar SR, Tyler JK (2004) Chromatin disassembly mediated by the histone chaperone Asf1 is essential for transcriptional activation of the yeast *PHO5* and *PHO8* genes. *Mol Cell* 14: 657–666. PMID: [15175160](#)
35. Adkins MW, Tyler JK (2006) Transcriptional activators are dispensable for transcription in the absence of Spt6-mediated chromatin reassembly of promoter regions. *Mol Cell* 21: 405–416. PMID: [16455495](#)
36. Shivaswamy S, Iyer VR (2008) Stress-dependent dynamics of global chromatin remodeling in yeast: dual role for SWI/SNF in the heat shock stress response. *Mol Cell Biol* 28: 2221–2234. doi: [10.1128/MCB.01659-07](#) PMID: [18212068](#)
37. Zabaronick SR, Tyler JK (2005) The histone chaperone anti-silencing function 1 is a global regulator of transcription independent of passage through S phase. *Mol Cell Biol* 25: 652–660. PMID: [15632066](#)
38. Zunder RM, Rine J (2012) Direct interplay among histones, histone chaperones, and a chromatin boundary protein in the control of histone gene expression. *Mol Cell Biol* 32: 4337–4349. doi: [10.1128/MCB.00871-12](#) PMID: [22907759](#)
39. Kristjuhan A, Svejstrup JQ (2004) Evidence for distinct mechanisms facilitating transcript elongation through chromatin *in vivo*. *EMBO J* 23: 4243–4252. PMID: [15457216](#)
40. Mellor J (2006) Dynamic nucleosomes and gene transcription. *Trends Genet* 22: 320–329. PMID: [16631276](#)
41. Ge Z, Wang H, Parthun MR (2011) Nuclear Hat1p complex (NuB4) components participate in DNA repair-linked chromatin reassembly. *J Biol Chem* 286: 16790–16799. doi: [10.1074/jbc.M110.216846](#) PMID: [21454479](#)
42. Mersfelder EL, Parthun MR (2008) Involvement of Hat1p (Kat1p) catalytic activity and subcellular localization in telomeric silencing. *J Biol Chem* 283: 29060–29068. doi: [10.1074/jbc.M802564200](#) PMID: [18753131](#)
43. Qin S, Parthun MR (2006) Recruitment of the type B histone acetyltransferase Hat1p to chromatin is linked to DNA double-strand breaks. *Mol Cell Biol* 26: 3649–3658. PMID: [16612003](#)
44. Green EM, Antczak AJ, Bailey AO, Franco AA, Wu KJ, et al. (2005) Replication-independent histone deposition by the HIR complex and Asf1. *Curr Biol* 15: 2044–2049. PMID: [16303565](#)
45. Huang S, Zhou H, Katzmann D, Hochstrasser M, Atanasova E, et al. (2005) Rtt106p is a histone chaperone involved in heterochromatin-mediated silencing. *Proc Natl Acad Sci U S A* 102: 13410–13415. PMID: [16157874](#)
46. Marheineke K, Krude T (1998) Nucleosome assembly activity and intracellular localization of human CAF-1 changes during the cell division cycle. *J Biol Chem* 273: 15279–15286. PMID: [9614144](#)
47. Verreault A, Kaufman PD, Kobayashi R, Stillman B (1996) Nucleosome assembly by a complex of CAF-1 and acetylated histones H3/H4. *Cell* 87: 95–104. PMID: [8858152](#)
48. Zhang H, Han J, Kang B, Burgess R, Zhang Z (2012) Human histone acetyltransferase 1 protein preferentially acetylates H4 histone molecules in H3.1-H4 over H3.3-H4. *J Biol Chem* 287: 6573–6581. doi: [10.1074/jbc.M111.312637](#) PMID: [22228774](#)
49. Silva AC, Xu X, Kim HS, Fillingham J, Kislinger T, et al. (2012) The replication-independent histone H3–H4 chaperones HIR, ASF1, and RTT106 co-operate to maintain promoter fidelity. *J Biol Chem* 287: 1709–1718. doi: [10.1074/jbc.M111.316489](#) PMID: [22128187](#)

50. Nair DM, Ge Z, Mersfelder EL, Parthun MR (2011) Genetic interactions between *POB3* and the acetylation of newly synthesized histones. *Curr Genet* 57: 271–286. doi: [10.1007/s00294-011-0347-1](https://doi.org/10.1007/s00294-011-0347-1) PMID: [21656278](https://pubmed.ncbi.nlm.nih.gov/21656278/)
51. Buurman ET, Jiang W, McCoy M, Averett DR, Thompson CM, et al. (2002) Validation of Cdc68p as a novel antifungal target. *Arch Microbiol* 178: 428–436. PMID: [12420162](https://pubmed.ncbi.nlm.nih.gov/12420162/)
52. Davis DA, Bruno VM, Loza L, Filler SG, Mitchell AP (2002) *Candida albicans* Mds3p, a conserved regulator of pH responses and virulence identified through insertional mutagenesis. *Genetics* 162: 1573–1581. PMID: [12524333](https://pubmed.ncbi.nlm.nih.gov/12524333/)
53. Al-Rawi N, Laforce-Nesbitt SS, Bliss JM (2010) Deletion of *Candida albicans* *SPT6* is not lethal but results in defective hyphal growth. *Fungal Genet Biol* 47: 288–296. doi: [10.1016/j.fgb.2010.01.001](https://doi.org/10.1016/j.fgb.2010.01.001) PMID: [20060921](https://pubmed.ncbi.nlm.nih.gov/20060921/)
54. Wysong DR, Christin L, Sugar AM, Robbins PW, Diamond RD (1998) Cloning and sequencing of a *Candida albicans* catalase gene and effects of disruption of this gene. *Infect Immun* 66: 1953–1961. PMID: [9573075](https://pubmed.ncbi.nlm.nih.gov/9573075/)
55. Lamarre C, LeMay JD, Deslauriers N, Bourbonnais Y (2001) *Candida albicans* expresses an unusual cytoplasmic manganese-containing superoxide dismutase (*SOD3* gene product) upon the entry and during the stationary phase. *J Biol Chem* 276: 43784–43791. PMID: [11562375](https://pubmed.ncbi.nlm.nih.gov/11562375/)
56. Ma LH, Takanishi CL, Wood MJ (2007) Molecular mechanism of oxidative stress perception by the Orp1 protein. *J Biol Chem* 282: 31429–31436. PMID: [17720812](https://pubmed.ncbi.nlm.nih.gov/17720812/)
57. Ardehali MB, Yao J, Adelman K, Fuda NJ, Petesch SJ, et al. (2009) Spt6 enhances the elongation rate of RNA polymerase II *in vivo*. *EMBO J* 28: 1067–1077. doi: [10.1038/emboj.2009.56](https://doi.org/10.1038/emboj.2009.56) PMID: [19279664](https://pubmed.ncbi.nlm.nih.gov/19279664/)
58. Baek YU, Kim YR, Yim HS, Kang SO (2004) Disruption of gamma-glutamylcysteine synthetase results in absolute glutathione auxotrophy and apoptosis in *Candida albicans*. *FEBS Lett* 556: 47–52. PMID: [14706824](https://pubmed.ncbi.nlm.nih.gov/14706824/)
59. Shahana S, Childers DS, Ballou ER, Bohovych I, Odds FC, et al. (2014) New Clox Systems for rapid and efficient gene disruption in *Candida albicans*. *PLoS One* 9: e100390. doi: [10.1371/journal.pone.0100390](https://doi.org/10.1371/journal.pone.0100390) PMID: [24940603](https://pubmed.ncbi.nlm.nih.gov/24940603/)
60. Hwang CS, Oh JH, Huh WK, Yim HS, Kang SO (2003) Ssn6, an important factor of morphological conversion and virulence in *Candida albicans*. *Mol Microbiol* 47: 1029–1043. PMID: [12581357](https://pubmed.ncbi.nlm.nih.gov/12581357/)
61. Chang P, Fan X, Chen J (2015) Function and subcellular localization of Gcn5, a histone acetyltransferase in *Candida albicans*. *Fungal Genet Biol*.
62. Lee JE, Oh JH, Ku M, Kim J, Lee JS, et al. (2015) Ssn6 has dual roles in *Candida albicans* filament development through the interaction with Rpd31. *FEBS Lett* 589: 513–520. doi: [10.1016/j.febslet.2015.01.011](https://doi.org/10.1016/j.febslet.2015.01.011) PMID: [25601565](https://pubmed.ncbi.nlm.nih.gov/25601565/)
63. Murad AM, Leng P, Straffon M, Wishart J, Macaskill S, et al. (2001) NRG1 represses yeast-hypha morphogenesis and hypha-specific gene expression in *Candida albicans*. *EMBO J* 20: 4742–4752. PMID: [11532938](https://pubmed.ncbi.nlm.nih.gov/11532938/)
64. Lionakis MS, Lim JK, Lee CC, Murphy PM (2011) Organ-specific innate immune responses in a mouse model of invasive candidiasis. *J Innate Immun* 3: 180–199. doi: [10.1159/000321157](https://doi.org/10.1159/000321157) PMID: [21063074](https://pubmed.ncbi.nlm.nih.gov/21063074/)
65. Majer O, Bourgeois C, Zwolanek F, Lassnig C, Kerjaschki D, et al. (2012) Type I interferons promote fatal immunopathology by regulating inflammatory monocytes and neutrophils during *Candida* infections. *PLoS Pathog* 8: e1002811. doi: [10.1371/journal.ppat.1002811](https://doi.org/10.1371/journal.ppat.1002811) PMID: [22911155](https://pubmed.ncbi.nlm.nih.gov/22911155/)
66. Benson LJ, Phillips JA, Gu Y, Parthun MR, Hoffman CS, et al. (2007) Properties of the type B histone acetyltransferase Hat1: H4 tail interaction, site preference, and involvement in DNA repair. *J Biol Chem* 282: 836–842. PMID: [17052979](https://pubmed.ncbi.nlm.nih.gov/17052979/)
67. Barman HK, Takami Y, Ono T, Nishijima H, Sanematsu F, et al. (2006) Histone acetyltransferase 1 is dispensable for replication-coupled chromatin assembly but contributes to recover DNA damages created following replication blockage in vertebrate cells. *Biochem Biophys Res Commun* 345: 1547–1557. PMID: [16735025](https://pubmed.ncbi.nlm.nih.gov/16735025/)
68. Fillingham J, Recht J, Silva AC, Suter B, Emili A, et al. (2008) Chaperone control of the activity and specificity of the histone H3 acetyltransferase Rtt109. *Mol Cell Biol* 28: 4342–4353. doi: [10.1128/MCB.00182-08](https://doi.org/10.1128/MCB.00182-08) PMID: [18458063](https://pubmed.ncbi.nlm.nih.gov/18458063/)
69. Schulz LL, Tyler JK (2006) The histone chaperone ASF1 localizes to active DNA replication forks to mediate efficient DNA replication. *FASEB J* 20: 488–490. PMID: [16396992](https://pubmed.ncbi.nlm.nih.gov/16396992/)
70. Umehara T, Chimura T, Ichikawa N, Horikoshi M (2002) Polyanionic stretch-deleted histone chaperone cia1/Asf1p is functional both *in vivo* and *in vitro*. *Genes Cells* 7: 59–73. PMID: [11856374](https://pubmed.ncbi.nlm.nih.gov/11856374/)

71. Stevenson JS, Liu H (2013) Nucleosome Assembly Factors CAF-1 and HIR Modulate Epigenetic Switching Frequencies in an H3K56 Acetylation-Associated Manner in *Candida albicans*. *Eukaryot Cell* 12: 591–603. doi: [10.1128/EC.00334-12](https://doi.org/10.1128/EC.00334-12) PMID: [23417560](https://pubmed.ncbi.nlm.nih.gov/23417560/)
72. Stillman B (1986) Chromatin assembly during SV40 DNA replication *in vitro*. *Cell* 45: 555–565. PMID: [3011272](https://pubmed.ncbi.nlm.nih.gov/3011272/)
73. De Backer MD, Ilyina T, Ma XJ, Vandoninck S, Luyten WH, et al. (2001) Genomic profiling of the response of *Candida albicans* to itraconazole treatment using a DNA microarray. *Antimicrob Agents Chemother* 45: 1660–1670. PMID: [11353609](https://pubmed.ncbi.nlm.nih.gov/11353609/)
74. Miyazaki T, Miyazaki Y, Izumikawa K, Takeya H, Miyakoshi S, et al. (2006) Fluconazole treatment is effective against a *Candida albicans* *erg3/erg3* mutant *in vivo* despite *in vitro* resistance. *Antimicrob Agents Chemother* 50: 580–586. PMID: [16436713](https://pubmed.ncbi.nlm.nih.gov/16436713/)
75. Tscherner M, Schwarzmüller T, Kuchler K (2011) Pathogenesis and Antifungal Drug Resistance of the Human Fungal Pathogen *Candida glabrata*. *Pharmaceuticals* 4: 169–186.
76. Prasad R, Rawal MK (2014) Efflux pump proteins in antifungal resistance. *Front Pharmacol* 5: 202. doi: [10.3389/fphar.2014.00202](https://doi.org/10.3389/fphar.2014.00202) PMID: [25221515](https://pubmed.ncbi.nlm.nih.gov/25221515/)
77. Perea S, Lopez-Ribot JL, Kirkpatrick WR, McAtee RK, Santillan RA, et al. (2001) Prevalence of molecular mechanisms of resistance to azole antifungal agents in *Candida albicans* strains displaying high-level fluconazole resistance isolated from human immunodeficiency virus-infected patients. *Antimicrob Agents Chemother* 45: 2676–2684. PMID: [11557454](https://pubmed.ncbi.nlm.nih.gov/11557454/)
78. Prasad R, De Wergifosse P, Goffeau A, Balzi E (1995) Molecular cloning and characterization of a novel gene of *Candida albicans*, *CDR1*, conferring multiple resistance to drugs and antifungals. *Curr Genet* 27: 320–329. PMID: [7614555](https://pubmed.ncbi.nlm.nih.gov/7614555/)
79. Sanglard D, Ischer F, Monod M, Bille J (1997) Cloning of *Candida albicans* genes conferring resistance to azole antifungal agents: characterization of *CDR2*, a new multidrug ABC transporter gene. *Microbiology* 143 (Pt 2): 405–416. PMID: [9043118](https://pubmed.ncbi.nlm.nih.gov/9043118/)
80. Sanglard D, Kuchler K, Ischer F, Pagani JL, Monod M, et al. (1995) Mechanisms of resistance to azole antifungal agents in *Candida albicans* isolates from AIDS patients involve specific multidrug transporters. *Antimicrob Agents Chemother* 39: 2378–2386. PMID: [8585712](https://pubmed.ncbi.nlm.nih.gov/8585712/)
81. Znaidi S, Barker KS, Weber S, Alarco AM, Liu TT, et al. (2009) Identification of the *Candida albicans* Cap1p regulon. *Eukaryot Cell* 8: 806–820. doi: [10.1128/EC.00002-09](https://doi.org/10.1128/EC.00002-09) PMID: [19395663](https://pubmed.ncbi.nlm.nih.gov/19395663/)
82. Kim HJ, Seol JH, Cho EJ (2009) Potential role of the histone chaperone, CAF-1, in transcription. *BMB Rep* 42: 227–231. PMID: [19403047](https://pubmed.ncbi.nlm.nih.gov/19403047/)
83. Ray-Gallet D, Woolfe A, Vassias I, Pellentz C, Lacoste N, et al. (2011) Dynamics of histone H3 deposition *in vivo* reveal a nucleosome gap-filling mechanism for H3.3 to maintain chromatin integrity. *Mol Cell* 44: 928–941. doi: [10.1016/j.molcel.2011.12.006](https://doi.org/10.1016/j.molcel.2011.12.006) PMID: [22195966](https://pubmed.ncbi.nlm.nih.gov/22195966/)
84. Ejlassi-Lassalette A, Mocquard E, Arnaud MC, Thiriet C (2010) H4 replication-dependent diacetylation and Hat1 promote S-phase chromatin assembly *in vivo*. *Mol Biol Cell* 22: 245–255. doi: [10.1091/mbc.E10-07-0633](https://doi.org/10.1091/mbc.E10-07-0633) PMID: [21118997](https://pubmed.ncbi.nlm.nih.gov/21118997/)
85. Suter B, Pogoutse O, Guo X, Krogan N, Lewis P, et al. (2007) Association with the origin recognition complex suggests a novel role for histone acetyltransferase Hat1p/Hat2p. *BMC Biol* 5: 38. PMID: [17880717](https://pubmed.ncbi.nlm.nih.gov/17880717/)
86. Lin LJ, Schultz MC (2011) Promoter regulation by distinct mechanisms of functional interplay between lysine acetylase Rtt109 and histone chaperone Asf1. *Proc Natl Acad Sci U S A* 108: 19599–19604. doi: [10.1073/pnas.1111501108](https://doi.org/10.1073/pnas.1111501108) PMID: [22106264](https://pubmed.ncbi.nlm.nih.gov/22106264/)
87. Bambach A, Fernandes MP, Ghosh A, Kruppa M, Alex D, et al. (2009) Goa1p of *Candida albicans* localizes to the mitochondria during stress and is required for mitochondrial function and virulence. *Eukaryot Cell* 8: 1706–1720. doi: [10.1128/EC.00066-09](https://doi.org/10.1128/EC.00066-09) PMID: [19717740](https://pubmed.ncbi.nlm.nih.gov/19717740/)
88. Thomas E, Roman E, Claypool S, Manzoor N, Pla J, et al. (2013) Mitochondria influence *CDR1* efflux pump activity, Hog1-mediated oxidative stress pathway, iron homeostasis, and ergosterol levels in *Candida albicans*. *Antimicrob Agents Chemother* 57: 5580–5599. doi: [10.1128/AAC.00889-13](https://doi.org/10.1128/AAC.00889-13) PMID: [23979757](https://pubmed.ncbi.nlm.nih.gov/23979757/)
89. Shingu-Vazquez M, Traven A (2011) Mitochondria and fungal pathogenesis: drug tolerance, virulence, and potential for antifungal therapy. *Eukaryot Cell* 10: 1376–1383. doi: [10.1128/EC.05184-11](https://doi.org/10.1128/EC.05184-11) PMID: [21926328](https://pubmed.ncbi.nlm.nih.gov/21926328/)
90. Gasch AP, Spellman PT, Kao CM, Carmel-Harel O, Eisen MB, et al. (2000) Genomic expression programs in the response of yeast cells to environmental changes. *Mol Biol Cell* 11: 4241–4257. PMID: [11102521](https://pubmed.ncbi.nlm.nih.gov/11102521/)
91. Chauhan N, Latge JP, Calderone R (2006) Signalling and oxidant adaptation in *Candida albicans* and *Aspergillus fumigatus*. *Nat Rev Microbiol* 4: 435–444. PMID: [16710324](https://pubmed.ncbi.nlm.nih.gov/16710324/)

92. MacCallum DM, Castillo L, Brown AJ, Gow NA, Odds FC (2009) Early-expressed chemokines predict kidney immunopathology in experimental disseminated *Candida albicans* infections. *PLoS One* 4: e6420. doi: [10.1371/journal.pone.0006420](https://doi.org/10.1371/journal.pone.0006420) PMID: [19641609](https://pubmed.ncbi.nlm.nih.gov/19641609/)
93. Sriskandan S, Altmann DM (2008) The immunology of sepsis. *J Pathol* 214: 211–223. PMID: [18161754](https://pubmed.ncbi.nlm.nih.gov/18161754/)
94. Zwolanek F, Riedelberger M, Stolz V, Jenull S, Istel F, et al. (2014) The non-receptor tyrosine kinase Tec controls assembly and activity of the noncanonical caspase-8 inflammasome. *PLoS Pathog* 10: e1004525. doi: [10.1371/journal.ppat.1004525](https://doi.org/10.1371/journal.ppat.1004525) PMID: [25474208](https://pubmed.ncbi.nlm.nih.gov/25474208/)
95. Mantegazza AR, Savina A, Vermeulen M, Perez L, Geffner J, et al. (2008) NADPH oxidase controls phagosomal pH and antigen cross-presentation in human dendritic cells. *Blood* 112: 4712–4722. doi: [10.1182/blood-2008-01-134791](https://doi.org/10.1182/blood-2008-01-134791) PMID: [18682599](https://pubmed.ncbi.nlm.nih.gov/18682599/)
96. Andaluz E, Ciudad T, Gomez-Raja J, Calderone R, Larriba G (2006) Rad52 depletion in *Candida albicans* triggers both the DNA-damage checkpoint and filamentation accompanied by but independent of expression of hypha-specific genes. *Mol Microbiol* 59: 1452–1472. PMID: [16468988](https://pubmed.ncbi.nlm.nih.gov/16468988/)
97. Lopes da Rosa J, Kaufman PD (2013) Chromatin-mediated *Candida albicans* virulence. *Biochim Biophys Acta* 1819: 349–355. PMID: [24459737](https://pubmed.ncbi.nlm.nih.gov/24459737/)
98. Lopez-Rubio JJ, Riviere L, Scherf A (2007) Shared epigenetic mechanisms control virulence factors in protozoan parasites. *Curr Opin Microbiol* 10: 560–568. PMID: [18024150](https://pubmed.ncbi.nlm.nih.gov/18024150/)
99. Hnisz D, Majer O, Frohner IE, Komnenovic V, Kuchler K (2010) The Set3/Hos2 histone deacetylase complex attenuates cAMP/PKA signaling to regulate morphogenesis and virulence of *Candida albicans*. *PLoS Pathog* 6: e1000889. doi: [10.1371/journal.ppat.1000889](https://doi.org/10.1371/journal.ppat.1000889) PMID: [20485517](https://pubmed.ncbi.nlm.nih.gov/20485517/)
100. Simonetti G, Passariello C, Rotili D, Mai A, Garaci E, et al. (2007) Histone deacetylase inhibitors may reduce pathogenicity and virulence in *Candida albicans*. *FEMS Yeast Res* 7: 1371–1380. PMID: [17627775](https://pubmed.ncbi.nlm.nih.gov/17627775/)
101. Smith WL, Edlind TD (2002) Histone deacetylase inhibitors enhance *Candida albicans* sensitivity to azoles and related antifungals: correlation with reduction in *CDR* and *ERG* upregulation. *Antimicrob Agents Chemother* 46: 3532–3539. PMID: [12384361](https://pubmed.ncbi.nlm.nih.gov/12384361/)
102. Wurtele H, Tsao S, Lepine G, Mullick A, Tremblay J, et al. (2010) Modulation of histone H3 lysine 56 acetylation as an antifungal therapeutic strategy. *Nat Med* 16: 774–780. doi: [10.1038/nm.2175](https://doi.org/10.1038/nm.2175) PMID: [20601951](https://pubmed.ncbi.nlm.nih.gov/20601951/)
103. Kaiser C, Michaelis S, Mitchell A (1994) *Methods in Yeast Genetics. A Laboratory Course Manual*. New York: Cold Spring Harbor Laboratory Press.
104. Gillum AM, Tsay EY, Kirsch DR (1984) Isolation of the *Candida albicans* gene for orotidine-5'-phosphate decarboxylase by complementation of *S. cerevisiae* *ura3* and *E. coli* *pyrF* mutations. *Mol Gen Genet* 198: 179–182. PMID: [6394964](https://pubmed.ncbi.nlm.nih.gov/6394964/)
105. Gacser A, Salomon S, Schafer W (2005) Direct transformation of a clinical isolate of *Candida parapsilosis* using a dominant selection marker. *FEMS Microbiol Lett* 245: 117–121. PMID: [15796988](https://pubmed.ncbi.nlm.nih.gov/15796988/)
106. Reuss O, Vik A, Kolter R, Morschhäuser J (2004) The SAT1 flipper, an optimized tool for gene disruption in *Candida albicans*. *Gene* 341: 119–127. PMID: [15474295](https://pubmed.ncbi.nlm.nih.gov/15474295/)
107. Krauke Y, Sychrova H (2011) Cnh1 Na(+)/H(+) antiporter and Ena1 Na(+)-ATPase play different roles in cation homeostasis and cell physiology of *Candida glabrata*. *FEMS Yeast Res* 11: 29–41. doi: [10.1111/j.1567-1364.2010.00686.x](https://doi.org/10.1111/j.1567-1364.2010.00686.x) PMID: [20942808](https://pubmed.ncbi.nlm.nih.gov/20942808/)
108. Hill JE, Myers AM, Koerner TJ, Tzagoloff A (1986) Yeast/*E. coli* shuttle vectors with multiple unique restriction sites. *Yeast* 2: 163–167. PMID: [3333305](https://pubmed.ncbi.nlm.nih.gov/3333305/)
109. Lee EC, Yu D, Martinez de Velasco J, Tessarollo L, Swing DA, et al. (2001) A highly efficient *Escherichia coli*-based chromosome engineering system adapted for recombinogenic targeting and subcloning of BAC DNA. *Genomics* 73: 56–65. PMID: [11352566](https://pubmed.ncbi.nlm.nih.gov/11352566/)
110. Zordan RE, Galgoczy DJ, Johnson AD (2006) Epigenetic properties of white-opaque switching in *Candida albicans* are based on a self-sustaining transcriptional feedback loop. *Proc Natl Acad Sci U S A* 103: 12807–12812. PMID: [16899543](https://pubmed.ncbi.nlm.nih.gov/16899543/)
111. Sedlazeck FJ, Rescheneder P, von Haeseler A (2013) NextGenMap: fast and accurate read mapping in highly polymorphic genomes. *Bioinformatics* 29: 2790–2791. doi: [10.1093/bioinformatics/btt468](https://doi.org/10.1093/bioinformatics/btt468) PMID: [23975764](https://pubmed.ncbi.nlm.nih.gov/23975764/)
112. Anders S, Pyl PT, Huber W (2015) HTSeq—a Python framework to work with high-throughput sequencing data. *Bioinformatics* 31: 166–169. doi: [10.1093/bioinformatics/btu638](https://doi.org/10.1093/bioinformatics/btu638) PMID: [25260700](https://pubmed.ncbi.nlm.nih.gov/25260700/)
113. Hnisz D, Bardet AF, Nobile CJ, Petryshyn A, Glaser W, et al. (2012) A histone deacetylase adjusts transcription kinetics at coding sequences during *Candida albicans* morphogenesis. *PLoS Genet* 8: e1003118. doi: [10.1371/journal.pgen.1003118](https://doi.org/10.1371/journal.pgen.1003118) PMID: [23236295](https://pubmed.ncbi.nlm.nih.gov/23236295/)

114. Robinson MD, McCarthy DJ, Smyth GK (2010) edgeR: a Bioconductor package for differential expression analysis of digital gene expression data. *Bioinformatics* 26: 139–140. doi: [10.1093/bioinformatics/btp616](https://doi.org/10.1093/bioinformatics/btp616) PMID: [19910308](https://pubmed.ncbi.nlm.nih.gov/19910308/)
115. Benjamini Y, Hochberg Y (1995) Controlling the False Discovery Rate: A Practical and Powerful Approach to Multiple Testing. *Journal of the Royal Statistical Society* 57: 289–300.
116. Oliveros JC (2007–2015) Venny. An interactive tool for comparing lists with Venn's diagrams.
117. Durchschlag E, Reiter W, Ammerer G, Schuller C (2004) Nuclear localization destabilizes the stress-regulated transcription factor Msn2. *J Biol Chem* 279: 55425–55432. PMID: [15502160](https://pubmed.ncbi.nlm.nih.gov/15502160/)
118. Veal EA, Toone WM, Jones N, Morgan BA (2002) Distinct roles for glutathione S-transferases in the oxidative stress response in *Schizosaccharomyces pombe*. *J Biol Chem* 277: 35523–35531. PMID: [12063243](https://pubmed.ncbi.nlm.nih.gov/12063243/)
119. Bourgeois C, Majer O, Frohner IE, Lesiak-Markowicz I, Hildering KS, et al. (2011) Conventional dendritic cells mount a type I IFN response against *Candida spp.* requiring novel phagosomal TLR7-mediated IFN-beta signaling. *J Immunol* 186: 3104–3112. doi: [10.4049/jimmunol.1002599](https://doi.org/10.4049/jimmunol.1002599) PMID: [21282509](https://pubmed.ncbi.nlm.nih.gov/21282509/)